Application of Geospatial Methodologies to Elucidate Honey bee (*Apis mellifera*) Colony Loss

by

Stephen Todd

A thesis submitted to the Graduate Faculty of
Auburn University
in partial fulfillment of the
requirements for the Degree of
Master of Science

Auburn, Alabama
August 6th, 2022

Approved by

Dr. Stephanie Rogers, Chair, Assistant Professor of Geosciences
Dr. Geoffrey Williams, Assistant Professor of Entomology and Plant Pathology
Dr. Todd Steury, Assistant Professor of Forestry and Wildlife Sciences

Abstract

Geospatial methods can be used in a wide variety of applications to elucidate interactions among variables across space and time and at various spatial scales. The identification of spatial trends is a foundational element of geospatial methods and can be determined through the use of spatial analysis. Honey bees (*Apis mellifera*) are a unique species for exploring geospatial methods as they are pervasive across the United States, have seen increasing losses in the past decade, and have complex interactions with their environment which are difficult to measure and understand across space and time. This thesis will explore how geospatial methods and spatial analysis assists in elucidating factors that may be leading to honey bee colony loss at various scales.

Chapter one of this thesis provides an overview of the main geographical, apicultural, and statistical concepts needed to understand the methods developed for this research. Specifically, spatial autocorrelation as measured using spatial statistics including the global and local Moran's *I*, honey bee colony loss as driven by *Varroa destructor*, and non-invasive colony inspection completed through thermal image capture.

Chapter two of this thesis aims to understand whether the abundance of *Varroa destructor*, a parasitic mite, shows clustering patterns at the national and regional scales using spatial statistics. *Varroa destructor* has been found to cluster spatially in New Zealand and Argentina, however spatial trends of *V. destructor* have not been investigated in the United States. Based on case studies in other countries, it was hypothesized that *V. destructor* spatial clustering will also be present in the United States. Spatial autocorrelation of *V. destructor* abundance was calculated using the global Moran's *I* and local Moran's *I* statistics, from both

manual and automated tasks in GIS. The results showed that *V. destructor* was spatial clustered in the United States and that the automated combination of the global and local Moran's *I* artificially inflates the detection of spatial clusters, and thus the manual calculation of the global and local Moran's *I* may be more appropriate.

Chapter three investigates the use of a thermal sensor on a drone to capture the average colony temperature and compare those temperatures with colony health metrics (number of adult bees, amount of brood, and amount of honey). I hypothesized that the sensor would capture the most accurate reading of average colony health with both lids removed and that the amount of brood and honey would significantly contribute to the average colony temperature. Data were collected in November 2020 and health metrics included the number of frames of adult bees, brood, honey, and the proportion of adults, brood, and honey in the top brood box. Thermal images were taken above 15 colonies with the outer and inner lid in place, the inner lid in place, and no lids. Backwards stepwise model building was used to identify variables with statistical significance as indicated by the *p*-value. Results indicate that the removal of the outer lid is most appropriate as it allows for the estimation of more honey bee health metrics and that a drone equipped with a thermal sensor can be used to conduct non-invasive colony health inspections.

Acknowledgments

I would first like to thank my advisor, Dr. Stephanie Rogers, for her continual guidance and support throughout my Master's program. I could not have undertaken this journey without her. She has been an inspiration and will be an example I look to as I continue to grow as an independent researcher. I am also thankful for my committee members, Dr. Geoffrey Williams and Dr. Todd Steury, for their feedback and support in my thesis. Moreover, I would like to recognize my fellow GeoIDEA lab members, specifically Edna Fernandez-Figueroa, Mallory Jordan, Kaj Overturf, Kelly Kaye, and Bethany Foust for their peer reviews and overall support. I am also so grateful for the wonderful friends I've made in the department. They have given me immense emotional support and been there for me on days when I did not think I could make it as a student. Lastly, special thanks to my parents, Linda and Steve, and girlfriend, Nora, who have supported me every step of the way. I would not be where I am today without their endless love and support. I would be remiss in not mentioning my cat, Cricket, for her many contributions, not only in my thesis, where she so eloquently stated "slkdfhkjlklkjlkjdskfkdsjf", but also in her attendance in every one of my zoom classes. Thank you to everyone.

I would also like to recognize that this research was completed at Auburn University in Lee County, Alabama. I recognize the forced removal of over 20,000 Muscogee Confederacy members by the United States army from Lee County and the surrounding area to Oklahoma in 1836 and 1837. I also recognize the sovereignty of the Muscogee Confederacy and celebrate their cultural past, present, and future.

Table of Contents

List of Tables

List of Figures

Chapter 1

Literature Review

1.1 Introduction

Since 2010 the average annual rate of honey bee (*Apis mellifera*) colony loss in the United States has been 39% (Bruckner et al. 2020; Steinhauer et al. 2014; vanEngelsdorp et al. 2008), with beekeepers most recently losing an estimated 44% of their colonies in 2020 (Bruckner et al. 2020) (Figure 1.1). Although annual colony loss is generally expected by beekeepers, especially over winter, acceptable losses range from 8-11%, which is far below the observed 44% (Kulhanek et al. 2017). Factors that contribute to these elevated rates of colony loss include inadequate beekeeper management practices (Steinhauer et al. 2014), weather and climate (Le Conte and Navajas 2008; Ali et al. 2019), pesticide use (Tosi et al. 2016), land-use change (Vaudo et al. 2012), and parasites including *Varroa destructor* (Le Conte et al. 2010; Traynor et al. 2020; Dooremalen et al. 2012). *Varroa destructor* is one of the main threats to honey bee populations (Beyer et al. 2018), and as a result, *V. destructor* threaten to accelerate the rate of honey bee colony loss and diminish the economic value of honey bees, which is valued annually at $14.2-$23.8 billion in the United States (Chopra et al. 2015) and $215 billion globally (Gallai et al. 2008). This economic value makes honey bees the third most important agricultural livestock in the world behind cattle and pork (Tautz 2008).

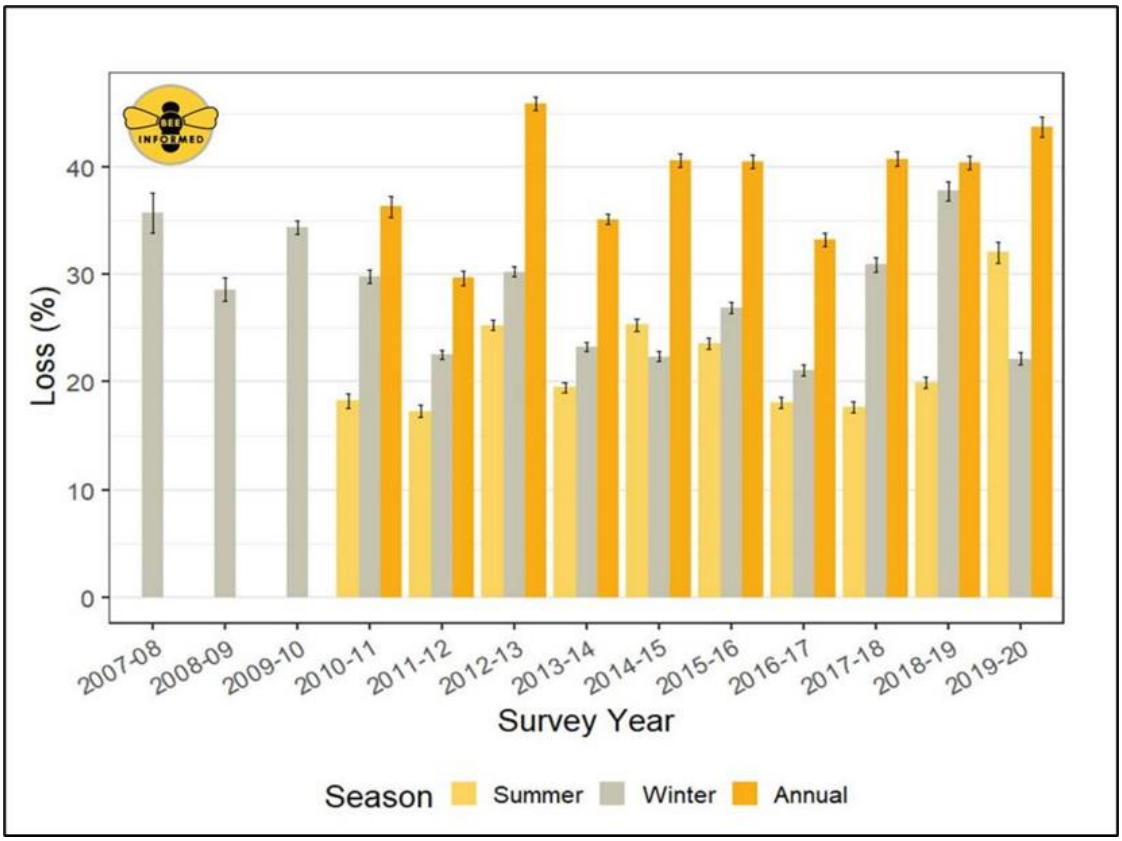

Figure 1.1 Summer, winter, and annual honey bee colony loss from 2007 to 2020. Total summer (April 1- October 1), winter (October 1- April 1), and annual (October 1-October 1) Honeybee (*Apis mellifera*) colony loss rates in the US across years of the Bee Informed Partnership's national honey bee colony loss survey (Bruckner et al. 2020).

1.2 Biological Background

1.2.1 Impacts of Varroa destructor on Honey Bees

Varroa destructor are obligate ectoparasites of honey bees and feed on the fat body of larvae and adult bees (Anderson and Truman 2000). At the individual level this feeding results in reduced body weight, malformation, and weakening of adults (Ramsey et al. 2019). At the colony level, moderate *V. destructor* infestation levels reduce the growth of honey bee populations, and therefore reduce honey production and winter survivorship (Dooremalen et al. 2012). At high infestation levels the colony will completely collapse within six to twenty-four months if left untreated (Le Conte et al. 2010).

In addition to the direct negative effect of *V. destructor* feeding, viral transmission driven by *V. destructor* also reduces honey bee populations and threatens colony survival (Sumpter and Martin 2004). The two viruses that have been confirmed to be vectored by *V. destructor* include deformed wing virus (DWV) (Martin and Brettell 2019) and acute bee paralysis virus (ABPV) (de Miranda et al. 2010). With the global spread of *V. destructor*, DWV now effects roughly 55% of colonies per apiary across 32 countries worldwide (Martin and Brettell 2019). Deformed wing virus is detrimental to honey bee health because it shortens the lifespan of adult bees to a few days, and colonies that tested positive for DWV had fewer combs of brood, which increased the likelihood of colony death the following winter (Martin 2001; Sumpter and Martin 2004). Similarly, *V. destructor* vector ABPV at 50-80% efficacy (Ball and Allen 1988) and adult bees that are infected with ABPV will experience rapid paralysis that includes darkening of hair on the thorax and abdomen, and an inability to fly, which results in death after a few days (de Miranda et al. 2010). At the colony level, ABPV infection is associated with decreased adult bee populations (Ball and Allen 1988).

1.2.2 Varroa destructor Distribution and Spread

Varroa destructor have been spread across the globe from southeast Asia since the 1960's and can now be found on all continents except Australia and Antarctica (Navajas 2010) (Figure 1.2). This spread can be traced back to the *V. destructor* host switch event from the Asian honey bee (*Apis cerana*) to the western honey bee in the 1950's (Akratanakul and Burgett 1975). This host switch event was facilitated by the introduction of western honey bee into Asia and is maintained because unlike the Asian honey bee, the western honey bee has adapted few defensive mechanisms, and as a result, *V. destructor* populations grow rapidly within western honey bee colonies (Braco et al. 1999; Kraus and Page 1995). These infested western honey bee

colonies were then shipped globally as part of the international trade of honey bees moving from Asia to Europe in the 1960's, to South America in the 1970's, and to South America and North America in the 1980's (Navajas 2010) (Figure 1.2).

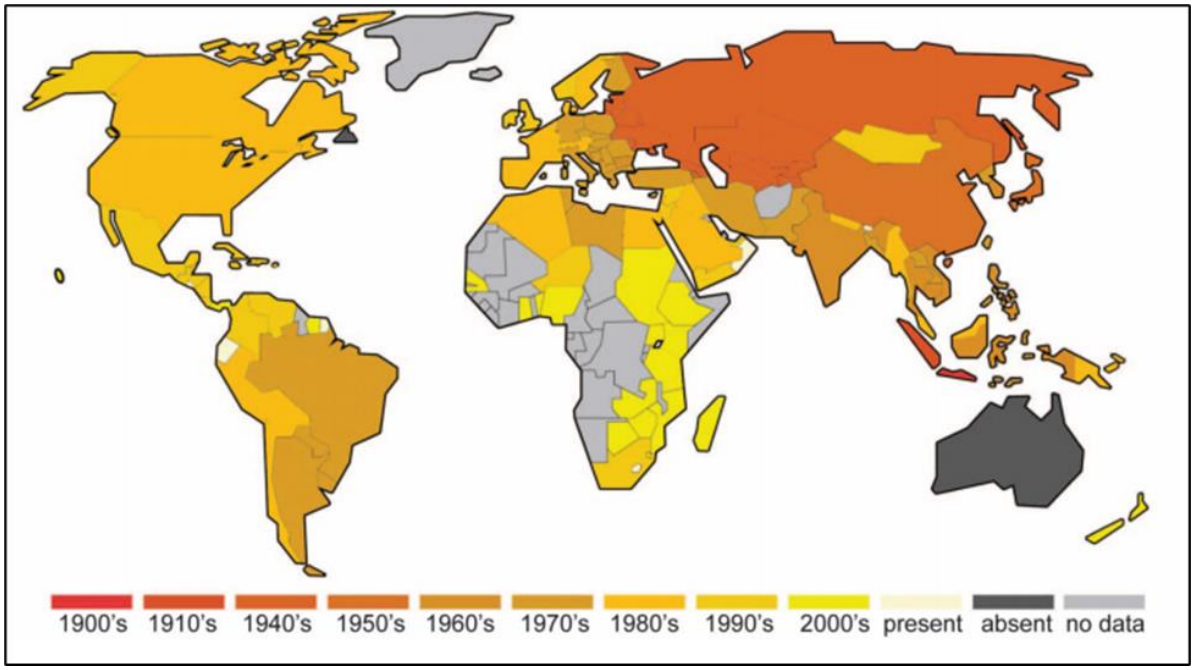

Figure 1.2 Spatial and Temporal spread of Varroa destructor from 1900 to present. Spatial and temporal spread of *Varroa destructor* in *Apis mellifera*, with more recent records of infestation shown in light yellow. Currently, the only remaining *Varroa destructor*-free land masses with substantial honey bee populations are Australia and Newfoundland (Wilfert et al. 2016).

1.2.3 Varroa destructor Monitoring and Management

The current *V. destructor* monitoring standard is to conduct an alcohol wash of ~300 adult worker bees and count the number of *V. destructor* that have been dislodged (Lee et al. 2010). The number of colonies to conduct alcohol washes varies on the size of the apiary with three colonies sampled recommended in four colony apiaries, and 8 colonies sampled recommended for >20 colony apiaries (Harris et al. 2019). If the presence of *V. destructor* is above 5% (15 mites/300 bees) treatment is recommended (Harris et al. 2019). Treatment strategies include acaricide application (Milani and Barbattini 1988; Milani and Lob 1998; Ritter

1988), organic acid or essential oil application (Calderone 1999; Calderone and Nasr 1999; Charrière and Imdorf 2002), and drone brood removal (Engels et al. 1984; Maul et al. 1988).

1.3 Spatial Background

1.3.1 Spatial Autocorrelation (Global Moran's I)

Spatial autocorrelation (SA) is a spatial statistic that builds upon Tobler's first law of geography, which states everything is related to everything else, but near things are more related than distant things (Tobler 1965). Spatial autocorrelation is the degree of similarity between georeferenced points or objects and is commonly measured using the global Moran's Index (*I)* statistic (Tobler 1965; Cliff and Ord 1973). The global Moran's index provides the sign and intensity of clustering, while the z-score and *p*-value indicate the significance of clustering. However, the global Moran's index does not indicate where clustering occurs across space. The global Moran's *I* statistic is calculated by:

$$I = \frac{n}{S_o} \frac{\sum_{i=1}^{n} \sum_{j=1}^{n} w_{i,j} z_i z_j}{\sum_{i=1}^{n} z_2^i} \quad (1)$$

where *I* is the global Moran's index, z_i is the deviation of an attribute for feature *i* from its mean, w_i, *j* is the spatial weight between feature *i* and *j*, *n* is equal to the total number of features, and S_o is the sum of all the spatial weights (Moran 1950). Spatial autocorrelation can either be positive or negative (Boots 2002; Nelson and Boots 2008). Positive SA occurs when similar values cluster together and the Moran's *I* index approaches +1, and negative SA occurs when dissimilar values cluster together and the Moran's *I* index approaches -1 (Cliff and Ord 1973). When the Moran's index is equal to 0, spatial randomness is present and therefore there is no SA and no clustering among features (Cliff and Ord 1973) (Figure 1.3). A Moran's *I* scatterplot quadrants

can be used to determine whether positive, negative, or no autocorrelation is present (Cliff and Ord 1973) (Figure 1.3). Within these scatterplot quadrants positive SA can be seen where similar values cluster (high-high and low-low), while negative SA can be seen where dissimilar values cluster (high-low and low-high).

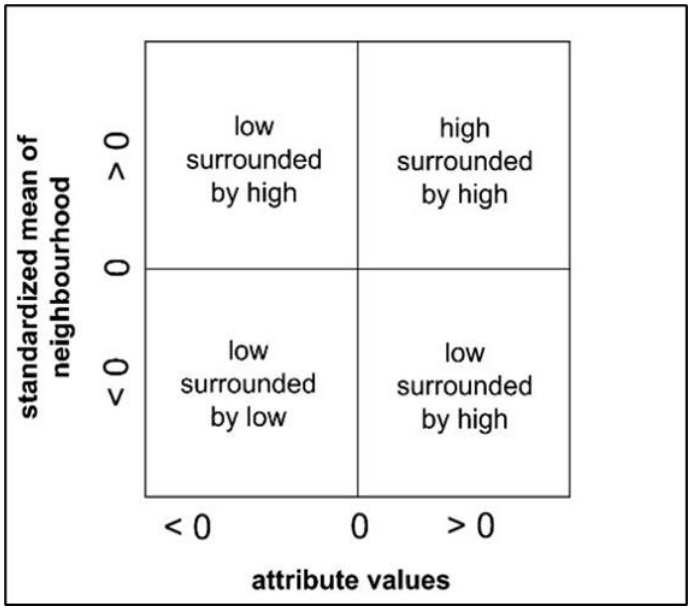

Figure 1.3. Moran's Scatter Plot. Moran scatter plot quadrants can be used to categorize locations based on the attribute value of a location in relation to the attribute values of neighbors. (Nelson and Boots 2008).

Spatial autocorrelation can also be either global, where one threshold is applied to the entire study area, or local, where variations in SA are calculated within subsets or neighborhoods of the study area (Cliff and Ord 1973). Global SA emphasizes typical distributions and assumes spatial uniformity throughout the study area (Boots 2002), however, if spatial uniformity is not held throughout the study area global SA will not represent the spatial patterns (Fotheringham 1997; Fotheringham and Brunson 1999). Application of the global Moran's *I* can indicate whether SA is present, whether the SA present is positive or negative, and the strength or significance of clustering, however, it cannot indicate where significant clusters are occurring.

1.3.2 Local Indicators of Spatial Autocorrelation

A local indicator of spatial autocorrelation (LISA) is any statistic that gives an indication of the extent of significant spatial clustering around an observation and is proportional to a global indicator of spatial association (Anselin 1995). The local Moran's *I* statistic is calculated by:

$$I_i = z_i \sum_j w_{ij} z_j \quad (2)$$

where the observations z_i, z_j are deviations from the mean for samples *i* and *j* (Anselin 1995). Unlike a global indicator of SA, a LISA provides spatially explicit information on where significant clustering occurs within a dataset, however, a LISA can still be compared with a global indicator through the comparison of z-scores.

Local indicators of spatial autocorrelation can be more appropriate than global indicators of SA when the spatial pattern is not uniform across the entire study area (Getis and Ord 2010). Local indicators of spatial autocorrelation can be compared to global indications of SA to understand whether the global statistic represents the average pattern of local autocorrelation (Anselin 1995). If the underlying process that is driving the spatial pattern is stable throughout space and time, then the local indicators would show little variation from the mean. But if local indicators significantly deviate from the mean then those regions would contribute more to the global statistic which, creates a global statistic that represents those areas of local significance, rather than the total dataset (Anselin 1995). A global statistic is problematic when determining the sign and strength of SA across a study area where spatial non-uniformity is present.

1.4 Application of Spatial Statistics in Entomological Systems

Kernel density estimation, which estimates a given value between fix points where the value has been measured, has been used to determine the point of introduction of *V. destructor* in New Zealand (Stevenson et al. 2005). Specifically, the presence of *V. destructor* at inspected colonies was used to estimate the presence of *V. destructor* between measured points. Moreover, because of the recent introduction of *V. destructor* in New Zealand the clustering of *V. destructor* presence indicated that those populations had been there longer, and thus the point of

introduction was determined to be the Auckland International Airport. Additionally, a spatial scan statistic similar to a LISA has been used to determine the clustering of *V. destructor* treatment failure in Argentina (Giacobino et al. 2016). They found that clusters of treatment failure were present within the country and that prior *V. destructor* infestation levels were positively correlated with treatment failure. This indirectly indicates that *V. destructor* population levels were also clustered, however, Giacobino et al. (2016) recommended further investigation.

Similar spatial statistics, including the global Moran's *I* (Moran 1950) and the local Moran's *I* (Anselin 1995), have been used to determine the clustering patterns of mountain pine beetles (*Dendroctonus ponderosae)* (Bone et al. 2013), mosquitos (*Aedes aegypti* L.) (Azil et al. 2014), and aphids (*Myzus persicae*) (Cocu et al. 2005), respectively. Specifically, Bone et al. (2013) applied a local bivariate Moran's *I*, which determined the risk classes and locations where mountain pine beetles were declining, increasing, or staying constant in British Columbia, Canada. Additionally, Azil et al. (2014) applied the global and local Moran's *I* to identify ideal trap type and locations for mosquitos at the neighborhood level in Australia. They found that although both trap types indicated SA, fewer BG-Sentinel traps could be used to maintain spatial accuracy. Lastly, Cocu et al. (2005) applied the local and global Moran's *I* on aphid populations in France and Great Britain and found that clustering of aphids was present.

1.5 Precision Apiculture

Precision agriculture is the use of technology to measure temporal and spatial trends to support management decisions in agricultural settings (Pierce and Nowak 1999). Precision apiculture is a subset of precision agriculture and specifically measures the temporal and spatial trends of honey bee colony health and thermoregulation to support management decisions

(Zacepins et al. 2012). Precision apiculture has employed the use of internal colony temperature sensors (Braga et al. 2020; Cook et al. 2021; Kridi et al. 2016; Meikle et al. 2015; Meikle et al. 2017), and thermal imagers (Bujok et al. 2002; Eskov and Toboev 2009; Eskov and Toboev 2011; Kleinhenz et al. 2003; Lim et al. 2013; Shaw et al. 2010) to measure the average temperature of honey bee colonies, which can be useful for estimating overall colony health. Specifically, Braga et al. (2020) integrated average colony temperature, ambient temperature, and colony health metrics measured in manual colony inspections to train a classification algorithm which predicted colony health status with 90% accuracy. Although average colony temperature, ambient temperature, and colony health metrics including the presence of adults, brood, and resources (pollen and honey) were included in the algorithm, no regression analysis was completed and thus the relationships among average colony temperature, and the presence of adults, brood, and resources was not determined. Regression analysis and the use of thermal imagers to measure the average colony temperature has been successful and found that the average colony temperature is positively correlated with the adult bee population (Shaw et al. 2010) and the winter survivorship of the colony (Lim et al. 2013).

Moreover, increased rates of honey bee colony loss underscore the need for regular colony inspections as they can provide early warning signs for complete colony loss including low populations of adults/brood, and low levels of resources. However, current manual colony inspections are time and labor intensive, and can disrupt the thermoregulation of the colony because of the invasive nature of the inspection. Non-invasive colony inspections have been investigated and include the measurement of the average colony temperature using external thermal imaging to estimate the adult bee population by regressing the average colony temperature and adult bee population. However, the application of drone technology is lacking in

precision apiculture, despite its widespread use in precision agriculture (Daponte et al. 2019), and thus the combination of drone and thermal technologies coupled with the inclusion of further honey bee health metrics should be explored.

1.6 Conclusion

Honey bee colony losses have been elevated in the United States since 2008 and threaten to diminish the economic production that honey bees provide through agricultural pollination services and honey production. Several drivers of honey bee colony loss have been identified; however, *V. destructor* are a key factor with higher infestation levels leading to increased loss. The identification of *V. destructor* infestation clusters has been completed in Argentina and New Zealand, however, no investigation to date has sought to identify them in the United States. Additionally, the successful application of the global and local Moran's *I* in entomological systems indicates that it can be applied to *V. destructor* infestation levels, and thus is the focus of Chapter two. Elevated rates of colony loss driven by *V. destructor* also underscore the importance of regular colony inspections. Current manual colony inspections are time and labor intensive, thus non-invasive colony inspections have been investigated through the application of thermal sensors. Precision apiculture allows for more regular colony inspection and therefore may curb elevated rates of colony loss. The combination of drone and thermal technologies coupled with the inclusion of further honey bee health metrics is the focus of Chapter three.

1.7 References

Akratanakul, P. & M. Burgett. 1975. “Varroa Jacobsoni: A Prospective Pest of Honeybees in Many Parts of the World.” *Bee World* 56 (3): 119-121. DOI: https://doi.org/10.1080/0005772X.1975.11097554.

Ali, H., A.S. Alqarni, J. Iqbal, A.A. Owayss, H.S. Raweh, and B.H. Smith. 2019. “Effect of Season and Behavioral Activity on the Hypopharyngeal Glands of Three Honey Bee *Apis mellifera* L. Races under Stressful Climatic Conditions of Central Saudi Arabia.” *Journal of Hymenoptera Research* 68: 85–101. DOI: https://doi.org/10.3897/jhr.68.29678.

Anderson, D.L., Trueman, J.W.H., 2000. “*Varroa jacobsoni* (*Acari*: *Varroidae*) is more than one species.” *Experimental and Applied Acarolo*gy 24: 165–189.

Anselin, L. 1995. “Local Indicators of Spatial Association-LISA.” *Geographical Analysis* 27 (2): 93–115. DOI: https://doi.org/10.1111/j.1538-4632.1995.tb00338.x.

Azil, A.H., D. Bruce, and C.R. Williams. 2014. “Determining the Spatial Autocorrelation of Dengue Vector Populations: Influences of Mosquito Sampling Method, Covariables, and Vector Control.” *Journal of Vector Ecology* 39 (1): 153–163. DOI: https://doi.org/10.1111/j.1948-7134.2014.12082.x.

Ball, B. V., and M. F. Allen. 1988. “The Prevalence of Pathogens in Honey Bee (*Apis mellifera*) Colonies Infested with the Parasitic Mite *Varroa Jacobsoni*.” *Annals of Applied Biology* 113 (2): 237–244. DOI: https://doi.org/10.1111/j.1744-7348.1988.tb03300.x.

Beyer, M., J. Junk, M. Eickermann, A. Clermont, F. Kraus, C. Georges, A. Reichart, and L. Hoffmann. 2018. “Winter Honey Bee Colony Losses, *Varroa destructor* Control Strategies, and the Role of Weather Conditions: Results from a Survey among Beekeepers.” *Research in Veterinary Science* 118: 52–60. DOI: https://doi.org/10.1016/j.rvsc.2018.01.012.

Bone, C., M.A. Wulder, J.C. White, C. Robertson, and T.A. Nelson. 2013. “A GIS-Based Risk Rating of Forest Insect Outbreaks Using Aerial Overview Surveys and the Local Moran’s I Statistic.” *Applied Geography* 40: 161–170. DOI: https://doi.org/10.1016/j.apgeog.2013.02.011.

Boots, B. 2002. “Local Measures of Spatial Association.” Ecoscience 9 (2): 168–76. DOI: https://doi.org/10.1080/11956860.2002.11682703.

Braco, M.R., N.A.C. Kidd, and R.S. Pickard. 1999. “Development of *Varroa jacobsoni* in Colonies of *Apis mellifera iberica* in a Mediterranean Climate.” Apidologie 30 (6): 491–503. DOI: https://doi.org/10.1051/apido:19990604.

Braga, A.R., D.G. Gomes, R. Rogers, E.E. Hassler, B.M. Freitas, J.A. Cazier. 2020. “A method for mining combined data from in-hive sensors, weather and apiary inspections to forecast the health status of honey bee colonies.” *Computers and Electronics in Agriculture* 169, 105161. DOI: https://doi.org/10.1016/j.compag.2019.105161.

Bruckner, S., N. Steinhauer, J. Engelsma, A.M. Fauvel, K. Kulhanek, E. Malcolm, A. Meredith, M. Milbrath, E.L. Niño, J. Rangel, K. Rennich, D. Reynolds, R. Sagili, J. Tsuruda, D. vanEngelsdorp, S.D. Aurell, M. Wilson, G. Williams. 2020. "2019-2020 Honey Bee Colony Losses in the United States: Preliminary Results."

Bujok, B., Kleinhenz, M., Fuchs, S., Tautz, J., 2002. Hot spots in the bee hive. *Naturwissenschaften* 89, 299–301. https://doi.org/10.1007/s00114-002-0338-7

Calderone, N.W., 1999. "Evaluation of formic acid and a thymol-based blend of natural products for the fall control of *Varroa jacobsoni* (*Acari: Varroidae*) in colonies of *Apis mellifera* (*Hymenoptera: Apidae*)." *Journal of Economic Entomology* 92: 253–260. DOI: https://doi.org/10.1093/jee/92.2.253.

Calderone, N.W., Nasr, M.E., 1999. "Evaluation of formic acid formulation for the fall control of *Varroa jacobsoni* (*Acari: Varroidae*) in colonies of the honey bee Apis mellifera (Hymenoptera: Apidae) in a temperate climate." *Journal of Economic Entomology* 92: 526–533. DOI: https://doi.org/10.1093/jee/92.3.526.

Charrière, J.D., and Imdorf, A. 2002. "Oxalic acid treatment by trickling against Varroa destructor: recommendations for use in central Europe and under temperate climate conditions." *Bee World* 83: 51–60. DOI: https://doi.org/10.1080/0005772X.2002.11099541.

Chopra, S.S., B.R. Bakshi, and V. Khanna. 2015. "Economic Dependence of U.S. Industrial Sectors on Animal-Mediated Pollination Service." *Environmental Science & Technology* 49 (24): 14441–14451. DOI: https://doi.org/10.1021/acs.est.5b03788.

Cliff, A.D. and Ord, J.K. 1973. Spatial autocorrelation. London: Pion.

Cocu, N., R. Harrington, M. Hulle, and M.D.A. Rounsevell. 2005. "Spatial Autocorrelation as a Tool for Identifying the Geographical Patterns of Aphid Annual Abundance." *Agricultural and Forest Entomology* 7 (1): 31–43. DOI: https://doi.org/10.1111/j.1461-9555.2005.00245.x.

Conte, Y. Le, and M. Navajas. 2008 "Climate Change: Impact on Honey Bee Populations and Diseases." *Revue scientifique et technique* 27(2): 499-510.

Conte, Y. Le, M. Ellis, and W. Ritter. 2010. "Varroa mites and Honey Bee Health: Can Varroa Explain Part of the Colony Losses?" *Apidologie* 41 (3): 353–363. DOI: https://doi.org/10.1051/apido/2010017.

Cook, D., Blackler, A., McGree, J., Hauxwell, C., 2021. Thermal Impacts of Apicultural Practice and Products on the Honey Bee Colony. *Journal of Economic Entomology* 114, 538–546. DOI: https://doi.org/10.1093/jee/toab023.

Daponte, P., L. De Vito, L. Glielmo, L. Iannelli, D. Liuzza, F. Picariello, G. Silano. 2019. "A review on the use of drones for precision agriculture." IOP Conference Services: Earth and Environmental Science 275, 012022. DOI: https://doi.org/10.1088/1755-1315/275/1/012022.

de Miranda, J.R., G. Corodoni, G. Budge. 2010. “The acute bee paralysis virus-kashmire bee virus-israeli acute paralysis virus complex.” *Journal of Invertebrate Pathology* 103: S30-S47. DOI: https://doi.org/10.1016/j.jip.2009.06.014.

Dooremalen, C. van, L. Gerritsen, B. Cornelissen, J.J.M. van der Steen, F. van Langevelde, and T. Blacquière. 2012. “Winter Survival of Individual Honey Bees and Honey Bee Colonies Depends on Level of Varroa destructor Infestation.” Edited by Mark F. Feldlaufer. *PLoS ONE* 7 (4): e36285. DOI: https://doi.org/10.1371/journal.pone.0036285.

Engels, W., Rosenkranz, P., Hertl, F., Staemmler, G., 1984. “Effect of drone brood removal on Varroa infested honey bee colonies.” *Apidologie* 15 (3): 246–248. DOI:

Eskov, E.K., Toboev, V.A., 2011. Seasonal dynamics of thermal processes in aggregations of wintering honey bees (Apis mellifera, Hymenoptera, Apidae). *Entomological Review* 91, 354–359. https://doi.org/10.1134/S0013873811030109.

Eskov, E.K., Toboev, V.A., 2009. Mathematical modeling of the temperature field distribution in insect winter clusters. *Biophysics* 54, 85–89. DOI: https://doi.org/10.1134/S000635090901014X.

Fotheringham, A. Stewart. 1997. “Trends in Quantitative Methods I: Stressing the Local.” *Progress in Human Geography* 21 (1): 88–96. DOI: https://doi.org/10.1191/030913297676693207.

Fotheringham, S., and C. Brunsdon. 1999. “Local Forms of Spatial Analysis.” *Geographical Analysis* 31 (4): 340-358. DOI: https://doi.org/10.1111/j.1538-4632.1999.tb00989.x.

Gallai, N., J.-M. Salles, J. Settele, and B.E. Vaissière. 2009. “Economic Valuation of the Vulnerability of World Agriculture Confronted with Pollinator Decline.” *Ecological Economics* 68 (3): 810–21. DOI: https://doi.org/10.1016/j.ecolecon.2008.06.014.

Getis, A., and J.K. Ord. 2010. “The Analysis of Spatial Association by Use of Distance Statistics.” *Geographical Analysis* 24 (3): 189–206. DOI: https://doi.org/10.1111/j.1538-4632.1992.tb00261.x.

Giacobino, A., A. Molineri, N. Bulacio Cagnolo, J. Merke, E. Orellano, E. Bertozzi, Germán M. 2016. “Key Management Practices to Prevent High Infestation Levels of Varroa Destructor in Honey Bee Colonies at the Beginning of the Honey Yield Season.” *Preventive Veterinary Medicine* 131: 95–102. DOI: https://doi.org/10.1016/j.prevetmed.2016.07.013.

Harris, J. W., J. R. Harbo, J. D. Villa, and R. G. Danka. 2003. “Variable Population Growth of Varroa destructor (Mesostigmata: Varroidae) in Colonies of Honey Bees (Hymenoptera: Apidae) During a 10-Year Period.” *Environmental Entomology* 32(6): 1305–12. DOI: https://doi.org/10.1603/0046-225X-32.6.1305.

Kleinhenz, M., Bujok, B., Fuchs, S., Tautz, J., 2003. “Hot bees in empty broodnest cells: heating from within.” *Journal of Experimental Biology* 206, 4217–4231. DOI: https://doi.org/10.1242/jeb.00680.

Kraus, B., and R. E. Page. 1995. “Population Growth of Varroa jacobsoni Oud in Mediterranean Climates of California.” *Apidologie* 26 (2): 149–157. DOI: https://doi.org/10.1051/apido:19950208.

Kridi, D.S., de Carvalho, C.G.N., Gomes, D.G., 2016. “Application of wireless sensor networks for beehive monitoring and in-hive thermal patterns detection.” *Computers and Electronics in Agriculture* 127, 221–235. DOI: https://doi.org/10.1016/j.compag.2016.05.013

Kulhanek, K., N. Steinhauer, K. Rennich, D.M. Caron, R.R. Sagili, J.S. Pettis, J.D. Ellis, M.E. Wilson, J.T. Wilkes, D.R. Tarpy, R. Rose, K. Lee, J. Rangel & D. vanEngelsdorp. 2017. “A national survey of managed honey bee2015–2016 annual colony losses in the USA.” *Journal of Apicultural Research* 56 (4): 328-340. DOI: https://doi.org/10.1080/00218839.2017.1344496.

Lee, K. V., R. D. Moon, E. C. Burkness, W. D. Hutchison, and M. Spivak. 2010. “Practical Sampling Plans for *Varroa destructor* (*Acari: Varroidae*) in *Apis mellifera* (*Hymenoptera: Apidae*) Colonies and Apiaries.” *Journal of Economic Entomology* 103(4): 1039–50. DOI: https://doi.org/10.1603/EC10037.

Lim, H.Y., J.G. Lee, S.B. Lee, O.M. Lee, B. Yoon. 2013. “Application of Digital Infrared Thermal Imaging (DITI) as a diagnostic method for the fate of honey bee colonies*.” Journal of Apiculture* 28 (2): 147-153.

Martin, S.J., and L.E. Brettell. 2019. “Deformed Wing Virus in Honeybees and Other Insects.” *Annual Review of Virology* 6 (1): 49–69. DOI: https://doi.org/10.1146/annurev-virology-092818-015700.

Martin, S.J. 2001. “The Role of Varroa and Viral Pathogens in the Collapse of Honeybee Colonies: A Modelling Approach: Collapse of Varroa -Infested Honeybee Colonies.” *Journal of Applied Ecology* 38 (5): 1082–93. DOI: https://doi.org/10.1046/j.1365-2664.2001.00662.x.

Maul, V., Klepsch, A., Assmannwerthmuller, U., 1988. “The trapping comb technique as part of bee management under strong infestation by Varroa jacobsoni Oud.” *Apidologie* 19 (2): 139–154. DOI:

Meikle, W.G., Weiss, M., Maes, P.W., Fitz, W., Snyder, L.A., Sheehan, T., Mott, B.M., Anderson, K.E., 2017. Internal hive temperature as a means of monitoring honey bee colony health in a migratory beekeeping operation before and during winter. *Apidologie* 48, 666–680. DOI: https://doi.org/10.1007/s13592-017-0512-8.

Meikle, W.G., Weiss, M., Stilwell, A.R., 2016. Monitoring colony phenology using within-day variability in continuous weight and temperature of honey bee hives. *Apidologie* 47, 1–14. DOI: https://doi.org/10.1007/s13592-015-0370-1.

Milani, N., and Barbattini, R., 1988. “Effectiveness of Apistan (Fluvalinate) in the control of Varroa jacobsoni Oudemans and its tolerance by Apis mellifera Linnaeus.” *Apicoltura* 4: 39–58. DOI: http://pascal-francis.inist.fr/vibad/index.php?action=getRecordDetail&idt=6657408.

Milani, N., Lob, M., 1998. “Plastic strips containing organophosphorous acaricides to control Varroa jacobsoni.” *American Bee Journal* 138: 612–615. DOI:

Moran, P.A. P. 1950. “Notes on Continuous Stochastic Phenomena.” *Biometrika* 37(1/2): 17–23. DOI: https://doi.org/10.2307/2332142.

Navajas, M.J. 2010. “Tracking the colonisation history of the invasive species Varroa destructor.” In: Sabelis M., Bruin J. (eds) *Trends in Acarology*. Springer, Dordrecht. DOI: https://doi.org/10.1007/978-90-481-9837-5_61.

Nelson, T.A., and B. Boots. 2008. “Detecting Spatial Hot Spots in Landscape Ecology.” *Ecography* 31 (5): 556–66. DOI: https://doi.org/10.1111/j.0906-7590.2008.05548.x.

Pierce, F.J., P. Nowak. 1999. “Aspects of Precision Agriculture, in: Advances in Agronomy.” *Elsevier*, pp. 1–85. DOI: https://doi.org/10.1016/S0065-2113(08)60513-1.

Ramsey, S.D., R. Ochoa, G. Bauchan, C. Gulbronson, J.D. Mowery, A. Cohen, D. Lim. 2019. “Varroa destructor Feeds Primarily on Honey Bee Fat Body Tissue and Not Hemolymph.” *Proceedings of the National Academy of Sciences* 116(5): 1792–1801. DOI: https://doi.org/10.1073/pnas.1818371116.

Ritter, W. 1981. “Varroa Disease of the Honeybee Apis Mellifera.” *Bee World* 62(4): 141-153. DOI: https://doi.org/10.1080/0005772X.1981.11097838.

Shaw, J.A., P.W. Nugent, J. Johnson, J.J. Bromenshenk, C.B. Henderson, S. Debnam. 2011. “Long-wave infrared imaging for non-invasive beehive population assessment.” *Optics Express* 19, 399. DOI: https://doi.org/10.1364/OE.19.000399.

Stehr, N.J. 2015. “Drones: The Newest Technology for Precision Agriculture.” *Natural Sciences Education* 44, 89–91. DOI: https://doi.org/10.4195/nse2015.04.0772.

Steinhauer, N.A, K. Rennich, M.E. Wilson, D.M. Caron, E.J. Lengerich, J.S. Pettis, R. Rose. 2014. “A National Survey of Managed Honey Bee 2012–2013 Annual Colony Losses in the USA: Results from the Bee Informed Partnership.” *Journal of Apicultural Research* 53 (1): 1–18. DOI: https://doi.org/10.3896/IBRA.1.53.1.01.

Stevenson, M.A., H. Benard, P. Bolger, and R.S. Morris. 2005. “Spatial Epidemiology of the Asian Honey Bee Mite (Varroa destructor) in the North Island of New Zealand.” *Preventive Veterinary Medicine* 71(3–4): 241–252. DOI: https://doi.org/10.1016/j.prevetmed.2005.07.007.

Sumpter, D. J. T., and S. J. Martin. 2004. “The Dynamics of Virus Epidemics in Varroa -Infested Honey Bee Colonies.” *Journal of Animal Ecology* 73 (1): 51–63. DOI: https://doi.org/10.1111/j.1365-2656.2004.00776.x.

Tautz, J. 2008. The buzz about bees: biology of a super-organism. Springer-Verlag Berlin Heidelberg.

Tobler, W.R. 1965. “Computation of the correspondence of geographical patterns.” Papers of the *Regional Science Association* 15: 131–139. DOI: https://doi.org/10.1007/BF01947869.

Tosi, S., F.J. Démares, S.W. Nicolson, P. Medrzycki, C.W.W. Pirk, and H. Human. 2016. “Effects of a Neonicotinoid Pesticide on Thermoregulation of African Honey Bees (Apis mellifera scutellata).” *Journal of Insect Physiology* 93–94: 56–63. DOI: https://doi.org/10.1016/j.jinsphys.2016.08.010.

Traynor, K.S., F. Mondet, J.R. de Miranda, M. Techer, V. Kowallik, M.A.Y. Oddie, P. Chantawannakul, and A. McAfee. 2020. “Varroa destructor: A Complex Parasite, Crippling Honey Bees Worldwide.” *Trends in Parasitology* 36 (7): 592–606. DOI: https://doi.org/10.1016/j.pt.2020.04.004.

vanEngelsdorp, D., J. Hayes, R.M. Underwood, and J. Pettis. 2008. “A Survey of Honey Bee Colony Losses in the U.S., Fall 2007 to Spring 2008.” Edited by Nick Gay. *PLoS ONE* 3 (12): e4071. DOI: https://doi.org/10.1371/journal.pone.0004071.

Vaudo, A.D., J.D. Ellis, G.A. Cambray, and M. Hill. 2012. “The Effects of Land Use on Honey Bee (Apis mellifera) Population Density and Colony Strength Parameters in the Eastern Cape, South Africa.” *Journal of Insect Conservation* 16 (4): 601–611. DOI: https://doi.org/10.1007/s10841-011-9445-0.

Wilfert, L., G. Long, H. C. Leggett, P. Schmid-Hempel, R. Butlin, S. J. M. Martin, and M. Boots. 2016. “Deformed Wing Virus Is a Recent Global Epidemic in Honeybees Driven by Varroa Mites.” *Science* 351 (6273): 594–97. DOI: https://doi.org/10.1126/science.aac9976.

Zacepins, A., E. Stalidzans, and J. Meitalovs. 2012. “Application of information technologies in precision apiculture.” In Proceedings of the 13th International Conference on Precision Agriculture (ICPA 2012).

Chapter 2

Identifying spatial clusters of a honey bee (*Apis mellifera*) parasite (*Varroa destructor*) in the United States from 2017 to 2020

2.1 Introduction

Honey bee (*Apis mellifera)* colony loss has reached significantly elevated levels in the Northern Hemisphere since 2008 (Oldroyd 2008). In the United States, the average annual rate of honey bee colony loss since 2010 has been 39% (Steinhauer et al. 2014; vanEngelsdorp et al. 2008), with beekeepers losing an estimated 44% of their colonies from April 2019 to April 2020 (Bruckner et al. 2020). Although annual loss is expected by beekeepers, acceptable losses due to the reduction of floral resources and inclement weather range from 8 to 11% (Kulhanek et al. 2017), which is far below the observed 44% of colony loss. Honey bee colony loss is significant because the economic value of honey bees, valued annually at $14.2-$23.8 billion in the United States (Chopra et al. 2015) and $215 billion globally (Gallai et al. 2008) making them the third most economically significant livestock in the world (Tautz 2008). Currently honey bees pollinate 52 out of the 115 leading crops in the world (Klein et al. 2007). Honey bees play a crucial role in agricultural production, with 22% of all agricultural production in developing nations and 14.7% of agricultural production in developed nations being directly pollinator dependent (Aizen et al., 2008). When indirect benefits from pollination are included, 35% of the human diet benefits from pollination (Klein et al. 2007).

Factors that contribute to increased honey bee colony loss include inadequate beekeeper management practices (Steinhauer et al. 2014), weather and climate (Ali et al. 2019; Beyer et al.

2018; Conte and Navajas 2008), pesticide use (Tosi et al. 2016), land-use change (Vaudo et al. 2012), and parasites, including *Varroa destructor* (Conte et al. 2010; Dooremalen et al. 2012; Traynor et al. 2020). *Varroa destructor* is an ectoparasite that was first found to parasitize the Eastern honey bee (*Apis cerana*) in Sumatra in 1904 (Oudemans 1904). Prior to the discovery of *V. destructor*, western honey bees were introduced into Asia in 1877 (Saiki and Okada 1973) and a period of sympatry continues to be shared between the eastern and western honey bee in Asia (Ruttner and Maul 1983). This period of sympatry mediated a host switch event, which occurred in the 1950's, when *V. destructor* was first found to parasitize the western honey bee (Delfinado 1963). Since the 1950's *V. destructor* has been inadvertently transported to all continents, except Australia and Antarctica, as part of the global honey bee trade and was introduced into North America in the mid-1980's (De Guzman et al. 1997). Currently, *V. destructor* can be found across the continental United States (Traynor et al. 2016) and poses a significant threat to honey bee colony health because the western honey bee have not co-evolved with the parasite, and thus western honey bees have less pronounced defense mechanisms against *V. destructor* than Eastern honey bees (Locke 2016). The susceptibility of Western bees to *V. destructor* requires beekeepers to closely monitor and manage for *V. destructor* (Kraus and Page 1995; Lee et al. 2010).

Varroa destructor threatens honey bee colony health by feeding on the fat body tissue of larvae and adult bees (Ramsey et al. 2019). This feeding results in reduced body weight, malformation, and overall weakening of adults (Ramsey et al. 2019). This feeding also vectors several viral diseases including deformed wing virus (Martin and Brettell 2019), and the acute bee paralysis virus (de Miranda et al. 2010), which also drive honey bee colony loss by shortening the lifespan of adults (Ball and Allen 1988; Carreck et al. 2010; Martin 2001;

Sumpter and Martin 2004). At the colony level, moderate infestation levels (<3 mites per 100 bees) reduce adult honey bee population growth, and therefore reduce honey production and winter survivorship (Dooremalen et al. 2012). At high infestation levels (>3 mites per 100 bees) colonies will collapse within one to three years if left untreated (Fries and Rosenkranz 1996; Ritter 1981). Although high infestation levels can be minimized through colony management and the application of pesticides (Delaplane et al. 2005; Fries et al. 1994), beekeepers may not apply similar management strategies and pesticides across space, leading to spatial clustering in *V. destructor* abundance (Giacobino et al. 2015). Thus, *V. destructor* populations may be more pervasive, in some areas of the country compared to others depending on the management strategies being applied by beekeepers. A study in New Zealand investigated whether the presence of *V. destructor* was spatially clustered using spatial statistics in the form of kernel density estimation to determine the point of introduction of *V. destructor* (Stevenson et al. 2005). They found a high level of *V. destructor*-positive colonies near the Auckland International Airport, which they identified as the point of introduction. In Argentina, it has been shown that spatial clusters of *V. destructor* treatment failure are present within the country and that these spatial clusters are significantly correlated with the level of *V. destructor* infestation prior to treatment, indicating that of the abundance of *V. destructor* populations may also be spatially clustered (Giacobino et al. 2016). Determination of *V. destructor* abundance clustering is significant because it allows beekeepers to appropriately adjust their monitoring and management strategies. The current recommendation in the United States for *V. destructor* monitoring is to survey ten percent of their colonies once per month from April to October (Cornell Cals 2020). If *V. destructor* infestation is above 3 mites per 100 bees it is recommended that treatment be applied in the form of acaricides or partial brood removal (Cornell Cals 2020),

however, beekeepers located within spatial clusters where *V. destructor* abundance is high the current *V. destructor* monitoring recommendation may need to be increased.

Spatial autocorrelation (SA), can be quantified using spatial statistics, including the global Moran's *I* (Moran 1950) and the local Moran's *I* (Anselin 1995). The global Moran's *I* statistic determines whether attributes of a sample in a study area are significantly clustered, dispersed, or spatially random by comparing the point values and the distance between them to the global mean (mean of all point values in a dataset) (Moran 1950). This generates the global Moran's *I* index, which indicates whether the attributes are clustered, dispersed, or spatially random (Moran 1950). For example, if the global Moran's index is close to one, the attributes are clustered, however, if the global Moran's index is close to negative one, the attributes are dispersed. Additionally, if the global Moran's index is close to zero, the attributes are spatially random. The significance of spatial clustering and dispersion is determined through the z-score and *p*-value. If the *p*-value is not significant, the null hypothesis of spatial randomness cannot be rejected, meaning the spatial distribution of some phenomena shows no spatial pattern and can be considered random. This means that if the Moran's index is not significant no clustering is present within the dataset. If the *p*-value is significant and the z-score is positive, the null hypothesis of spatial randomness can be rejected, and clustering of similar values is present. If the *p*-value is significant and the z-score is negative the null hypothesis of spatial randomness can be rejected, and spatial dispersion is present. Although the global Moran's *I* statistic determines whether clustering is present within attributes, it does not indicate where clustering is located (Moran 1950).

To determine where clustering of similar values is present across space, a local indicator of spatial autocorrelation (LISA) in the form of the local Moran's *I* statistic (Anselin 1995) can

be used. Like the global Moran's *I* statistic, the local Moran's *I* determines whether point values are clustered, dispersed, or spatially random, but instead of a global mean it compares the point values to the local mean (mean of values within a given area of the dataset) (Anselin 1995).

However, the local Moran's *I* is a neighborhood size dependent equation (Anselin 1995), and an appropriate neighborhood size must be determined for each novel application (Nelson and Boots 2008). The area where the local mean is calculated is the spatial neighborhood. The neighborhood distance where spatial autocorrelation is strongest can be determined by calculating the local Moran's index at increasing neighborhood sizes. The nearest distance at which the z-score is largest (first peak) is the appropriate neighborhood size (ESRI 2022).

Once the appropriate neighborhood size has been identified the local Moran's *I* generates a local Moran's index. If the point value is high and the local mean is similarly high the point will be identified as a high cluster, however, if the point value is low and the local mean is similarly low the point will be identified as a low cluster (Anselin 1995). Additionally, if the point value is high and the local mean is low, or if the point value is low and the local mean is high, the point will be identified as an outlier.

The global and local Moran's *I* statistics have been used in a wide variety of spatial epidemiological applications to measure spatial autocorrelation and determine clustering patterns of pest insects including mountain pine beetles (*Dendroctonus ponderosae)* (Bone et al. 2013), mosquitos (*Aedes aegypti L.*) (Azil et al. 2014), and aphids (*Myzus persicae*) (Cocu et al. 2005). To determine the appropriate neighborhood size for understanding clustering of mosquito abundance, Azil et al. (2014) applied the local Moran's *I* at increasing neighborhood sizes, and the neighborhood size where clustering was most pronounced, as indicated by the highest z-score and associated significant relationships as determined by *p*-values, identified the appropriate

neighborhood size, in that case the neighborhood size was 40 meters.

Although the manual application of the global Moran's *I,* incremental spatial autocorrelation, and the local Moran's *I* can uncover the clustering patterns of insect abundance, optimized outlier analysis automatically combines incremental spatial autocorrelation and the local Moran's *I.* Optimized outlier analysis also includes locational outlier detection and removal. Locational outliers are features that are much farther away from neighboring features than the majority of features in the dataset. Locational outliers are computed by calculating the average nearest neighbor distance for each feature and evaluating the distribution of all of these distances. Features that are more than a three standard deviation distance away from their closest noncoincident neighbor are considered locational outliers (ESRI 2022). Additionally, the optimized outlier analysis will calculate the optimal neighborhood size by calculating the incremental spatial autocorrelation and identify a z-score peak. When a z-score peak cannot be identified the average distance to 30 neighbors is calculated and used as the appropriate neighborhood size. The optimal outlier analysis will then calculate the local Moran's *I* and identify high-high clusters, low-low clusters, high-low outliers, low-high outliers, and non-significant points.

Varroa destructor abundance in the United States presents an opportunity to determine whether the inclusion of locational outliers and calculating the average distance to 30 neighbors when a z-score peak cannot be identified in the optimized outlier analysis increases the detection of high-high and low-low clusters, respectively. Determining whether optimized outlier analysis increases the detection of high-high and low-low clusters is significant because the tool may be used and artificially inflate the detection of clusters, thus biasing the results of those who use it. Therefore, I hypothesize that *V. destructor* infestation levels are spatially autocorrelated in the

United States from 2017 to 2020, and that the inclusion of locational outliers and calculating the average distance to 30 neighbors when a z-score peak cannot be identified increases the detection of high-high and low-low clusters, respectively.

2.2 Methods

2.2.1 Data

Data were obtained from MiteCheck, a national scale citizen science survey which has collected *V. destructor* infestation data on an on-going basis since 2015 (MiteCheck 2021). MiteCheck represents the most robust national scale dataset on *V. destructor* infestation levels in the United States, with 3,904 survey entries spanning from 2015 to 2021. This online survey asks beekeepers for their contact information, apiary location in geographic coordinates, which (if any) *V. destructor* control methods were used within the past two months, if control methods will be used in the next two months, sample collection date, survey method, and *V. destructor* infestation level per 100 bees.

2.2.2. Data Preparation

A subset of data were extracted from the MiteCheck dataset. This subset encompassed 3,765 survey entries in the contiguous United States from 2017 to 2020. Data from 2015, 2016, and 2021 were removed because the low sample size within each year (1 survey in 2015, 482 surveys in 2016, and 19 surveys in 2021, respectively). Data from 2017 to 2020 were subdivided for each year, and for the month of September in the years of 2017, 2018, and 2019 as they represented the timeframes when most surveys were completed and allowed for more robust applications of the global and local Moran's *I* statistic (Table 2.1). September was the month when most surveys were submitted to MiteCheck as beekeepers are encouraged to submit surveys in late August and early September as part of their Mite-a-thon initiative (Mitecheck

2021). Also, September represents a critical time for beekeepers to survey their colonies because overwinter survival has been linked to the level of *V. destructor* infestation in late summer (Giacobino et al. 2014). Where multiple surveys were completed at the same location within the same month or year, the mean infestation levels were calculated by summing the number of *V. destructor* per 100 bees and dividing by the number of colonies surveyed to produce a single *V. destructor* infestation level to avoid pseudoreplication (Millar and Anderson 2004).

Table 2.1 Subdivisions of MiteCheck data reported by time period. Apiary locations represent the total number of apiary locations submitted by beekeepers. Bad records represent invalid data that were not readable by ArcGIS Pro. Input number of features represent apiary locations minus bad records.

Time period	Apiary locations	Bad records	Input number of features
2017	1,171	0	1,171
2018	1,527	21	1,506
2019	1,807	708	1,099
2020	1,363	0	1,363
Sept. 2017	952	0	952
Sept. 2018	793	9	784
Sept. 2019	739	200	539

2.2.3 Global Moran's I

The global Moran's *I* statistic was calculated for each of the seven data subdivisions (Table 2.1) using the *Spatial Autocorrelation* (global Moran's *I*) tool in ArcGIS Pro 2.8 (Figure 2.1). The global Moran's *I* statistic is calculated by:

$$I = \frac{n}{S_o} \frac{\sum_{i=1}^{n} \sum_{j=1}^{n} w_{i,j} z_i z_j}{\sum_{i=1}^{n} z_2^i} \quad (1)$$

where *I* is the global Moran's index, z_i is the deviation of an attribute for feature *i* from its mean, $w_{i,j}$ is the spatial weight between feature *i* and *j*, *n* is equal to the total number of features, and S_o

is the sum of all the spatial weights (Moran 1950). For this analysis, *V. destructor* infestation level was the attribute of colony *i,* and inverse distance was used as the spatial weight between colony *i* and *j* as it assigns higher spatial weight to colonies that are closer together than those that are farther apart. The total number of colonies (*n*) was populated with the corresponding values for each input data subdivision (Table 2.1), and the sum of all spatial weights (S_o) was generated by the *Spatial Autocorrelation* tool. Lastly, Euclidean (straight-line) distance was used as the definition of distance because the transmission of *V. destructor* is not constrained to transportation (network distance) or grids (Manhattan distance).

2.2.4 Determining Neighborhood Size

For each subdivision of data that had a statistically significant positive global Moran's *I* index (Table 2.2) indicating that the data were spatially autocorrelated, the optimal neighborhood size where clustering was maximized was calculated using the *Incremental Spatial Autocorrelation* tool (Figure 2.1). For this analysis, twenty distance bands (the maximum allowed) increasing at the default distance increment automatically calculated by ArcGIS Pro were used to determine the optimal neighborhood size across a broad spatial scale while maintaining high spatial resolution.

2.2.5 Local Indicator of Spatial Autocorrelation

The *Cluster and Outlier analysis* (local Moran's *I*) tool was applied to determine where clustering of high *V. destructor* infestation values, clustering of low *V. destructor* infestation values, and statistical outliers, occurred (Figure 2.1). The local Moran's *I* statistic is calculated by:

$$I_i = z_i \sum_j w_{ij} \times z_j \qquad (2)$$

where the observations z_i, z_j are deviations from the mean *j* (Anselin 1995). Similar to the global Moran's *I* statistic, *V. destructor* infestation level was used as feature *i*, inverse distance was used as the definition of spatial weighting between features *i* and *j*, Euclidean was used as the definition of distance, and the neighborhood size was set as the distance where clustering was most pronounced among the data (first Moran's *I* z-score peak) resulting from the *Incremental Spatial Autocorrelation* tool. A new subdivision of data was generated which displayed whether each apiary location belonged to a high-high cluster, a low-low cluster, a statistical outlier (low-high or low-high), or a point of non-significance.

2.2.6 Optimized Outlier Analysis

The *optimized outlier analysis* tool combines and automates the calculation of the *Incremental spatial autocorrelation* tool and local Moran's *I.* The *optimized outlier analysis* tool was applied to all subdivision of data that had a significantly positive global Moran's index value (Figure 2.1).

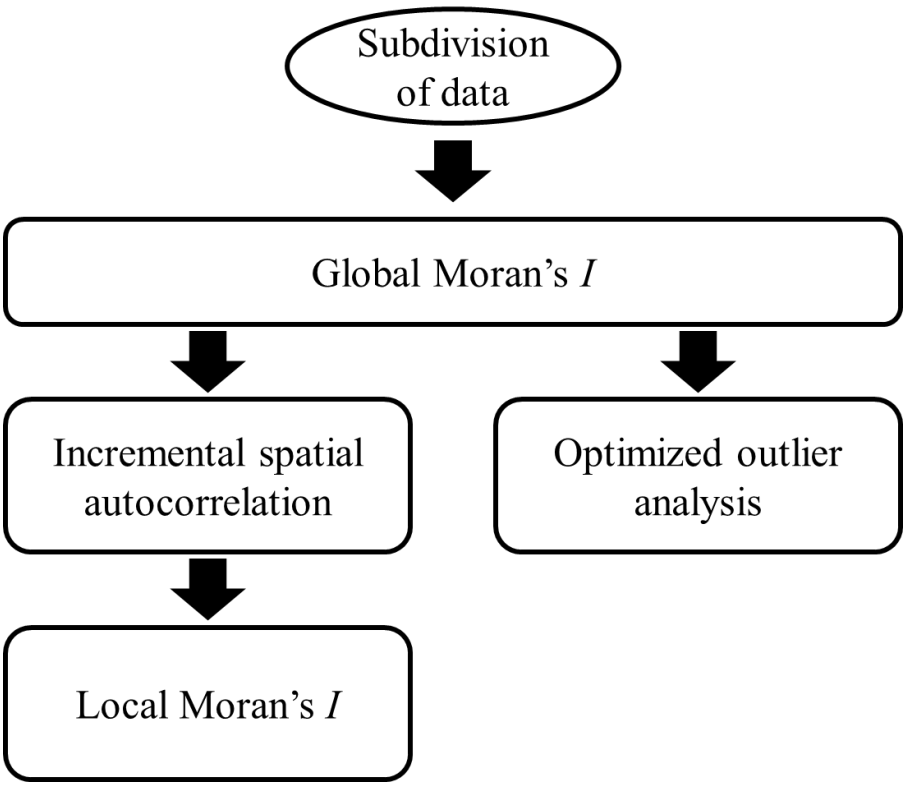

Figure 2.1 Analytical workflow within ArcGIS Pro. The workflow begins with a subdivision of MiteCheck data. The global Moran's *I* is calculated for that subdivision. If the global Moran's index is significantly positive the incremental spatial autocorrelation tool was manually applied. Where spatial clustering was most significant the local Moran's *I* was then calculated. Alternatively, if the global Moran's index was significantly positive the optimized outlier analysis was applied.

2.3 Results

2.3.1 Global Moran's I

In 2017 1,171 apiary locations were submitted to MiteCheck with zero bad records included resulting in 1,171 input features. The Moran's index was 0.009 with a of variance of 0.00003, z-score of 1.72, and *p*-value of 0.085. The combination of the z-score and *p*-value resulted in a SA status of clustered. In 2018 1,527 apiary locations were submitted to MiteCheck with 21 bad records included resulting in 1,506 input features. The Moran's index was 0.24 with a variance of 0.0002, z-score of 16.16, and *p*-value of <0.01. The combination of the z-score and *p*-value resulted in a SA status of clustered. In 2019 1,807 apiary locations were submitted to

MiteCheck with 798 bad records included resulting in 1,099 input features. The Moran's index was 0.47 with a variance of 0.0003, z-score of 25.96, and a *p*-value of <0.01. The combination of the z-score and *p*-value resulted in a SA status of clustered. In 2020 1,363 apiary locations were submitted to MiteCheck with zero bad records resulting in 1,363 input features. The Moran's index was 0.05 with a variance of 0.0003, z-score of 2.85, and a *p*-value of <0.01. The combination of the z-score and the *p*-value resulted in a SA status of clustered. In September of 2017 952 apiary locations were submitted to MiteCheck with zero bad records resulting in 952 input features. The Moran's index was 0.03 with a variance of 0.00006, z-score of 4.1, and a *p*-value of <0.01. The combination of the z-score and *p*-value resulted in a SA of clustered. In September of 2018 793 apiaries were submitted to MiteCheck with 9 bad records resulting in 784 input features. The Moran's index was 0.018 with a variance of 0.00014, z-score of 1.61, and a *p*-value of 0.11. The combination of the z-score and *p*-value resulted in a SA status of spatially random. In September of 2019 739 apiary locations were submitted to MiteCheck with 200 bad records resulting in 539 input features. The Moran's index was 0.14 with a variance of 0.0004, z-score of 7.84, and a *p*-value of <0.01. The combination of the z-score and *p*-value resulted in a SA status of clustered.

Time period	Apiary locations	Bad records	Input number of features	Moran's index	Variance	z-score	*p* -value	Spatial autocorrelation status
2017	1,171	0	1,171	0.01	0.00003	1.72	0.08	Clustered
2018	1,527	21	1,506	0.24	0.00022	16.16	<0.01	Clustered
2019	1,807	708	1,099	0.47	0.00033	25.96	<0.01	Clustered
2020	1,363	0	1,363	0.05	0.00029	2.85	<0.01	Clustered
Sept. 2017	952	0	952	0.03	0.00006	4.10	<0.01	Clustered
Sept. 2018	793	9	784	0.02	0.00014	1.61	0.11	Random
Sept. 2019	739	200	539	0.14	0.00035	7.84	<0.01	Clustered

Table 2.2 Results of the global Moran's *I* of *Varroa destructor* abundance in from 2017 to 2020 and in September of 2017, 2018, and 2019. Apiary locations represent the number of apiary locations. Bad records represent the number of invalid surveys. Input features is the final value with bad records removed. The Moran's index is the level of spatial autocorrelation present within the dataset. Variance is the measure of the spread of the data with smaller values indicating a smaller spread from the mean. Z-score is the difference between the feature value and the global mean measured in standard deviations. The *p*-value is the probability of obtaining test results at least as extreme as the result actually observed, under the assumption that the null hypothesis is correct. When the *p*-value is non-significant spatial randomness is present. When the *p*-value is significant and the z-score is positive spatial clustering is present. When the *p*-value is significant and the z-score is negative spatial dispersion is present.

2.3.2 Neighborhood size

In 2017 the default start distance was 341.2 km increasing by 20.7 km. The first z-score peak was 507.5 km while the maximum z-score peak was 673.3 km (Figure 2.2). In 2018 the default start distance was 273.9 km increasing by 54.8 km. The first z-score peak was 328.9 km while the maximum z-score peak was 493 km (Figure 2.3). In 2019 the default start distance was 261.4 km increasing by 52.3 km, however, neither a first z-score peak nor a maximum z-score peak was identified (Figure 2.4). In 2020 the default start distance was 344.3 km increasing by 16.4 km. The first z-score was 360.7 km while the maximum z-score peak was 442.6 km (Figure 2.5). In September of 2017 the default start distance was 341.8 km increasing by 22.8 km. The first z-score peak was 524.1km while the maximum z-score peak was 683.7 km (Figure 2.6). September of 2018 was found to be spatially random, and thus the *Incremental spatial autocorrelation* tool was not applied (Table 2.2). In September of 2019 the default start distance was 272.6 km increasing by 54.5 km, however, neither a first z-score peak nor a maximum z-score peak was identified (Figure 2.7).

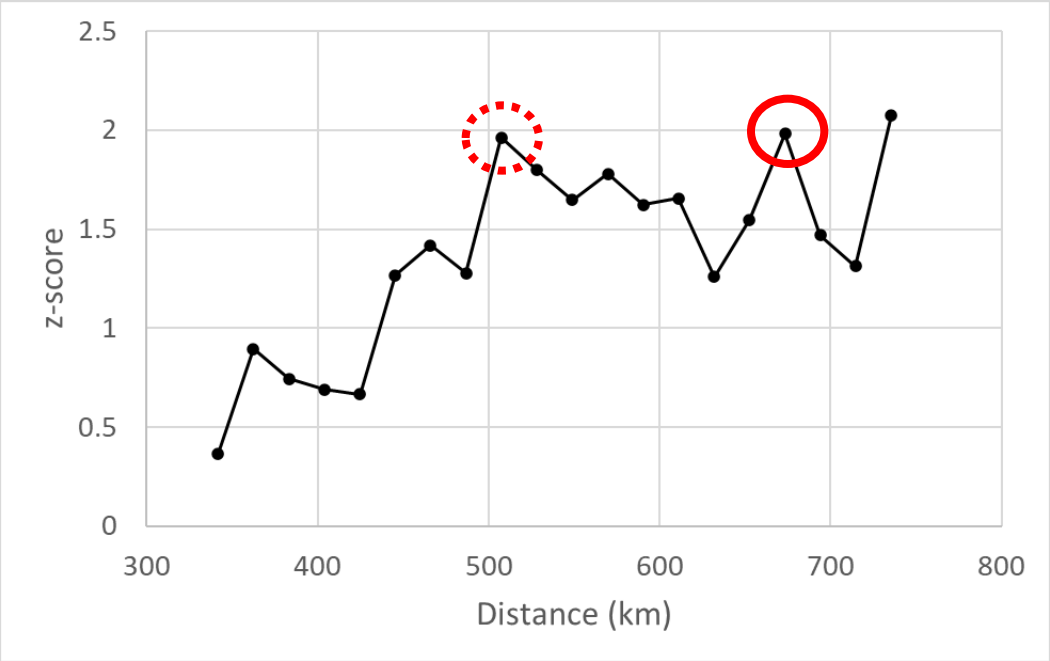

Figure 2.2 Results of Incremental Spatial Autocorrelation of *Varroa destructor* abundance in 2017. The default start distance was 341.2 km increasing by 20.7 km. The first z-score identified in the dashed circle was 507.5 km with the maximum z-score identified in the solid circle being 673.3 km.

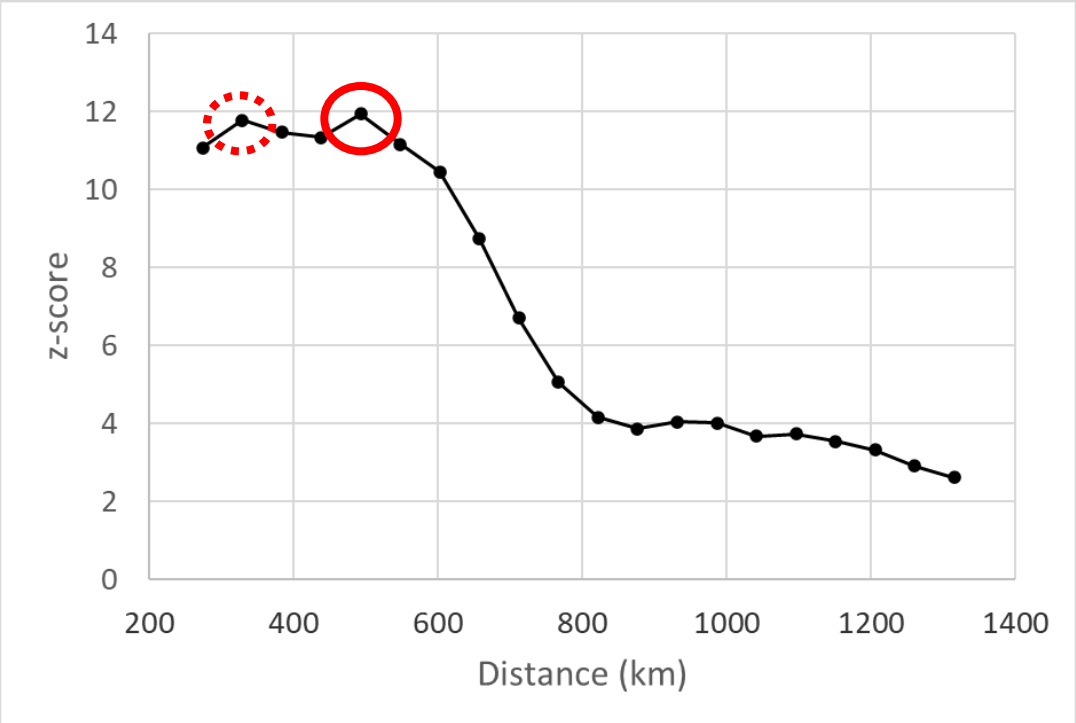

Figure 2.3 Results of Incremental Spatial Autocorrelation of *Varroa destructor* abundance in 2018. The default start distance was 273.9 km increasing by 54.7 km. The first z-score identified in the dashed circle was 328.9 km with the maximum z-score identified in the solid circle being 493 km.

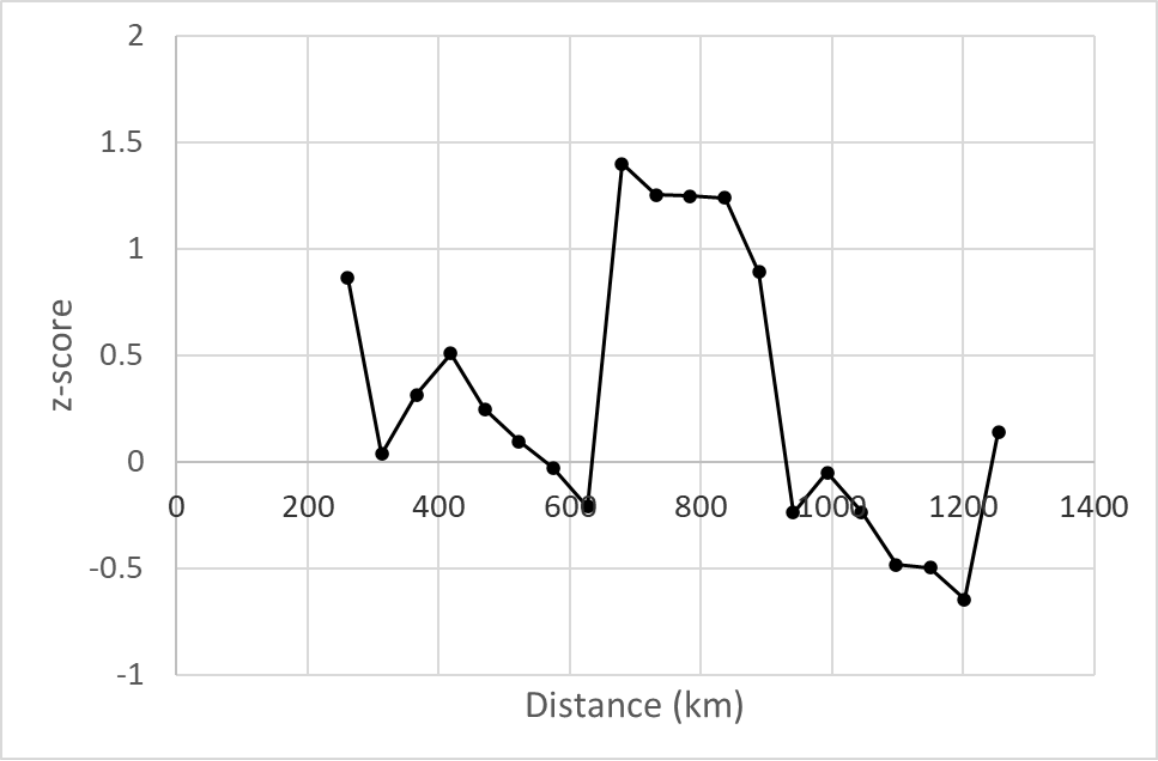

Figure 2.4 Results of Incremental Spatial Autocorrelation of *Varroa destructor* abundance in 2019. The default start distance was 261.4 km increasing by 52.3 km. Neither a first z-score peak nor a maximum z-score peak was identified.

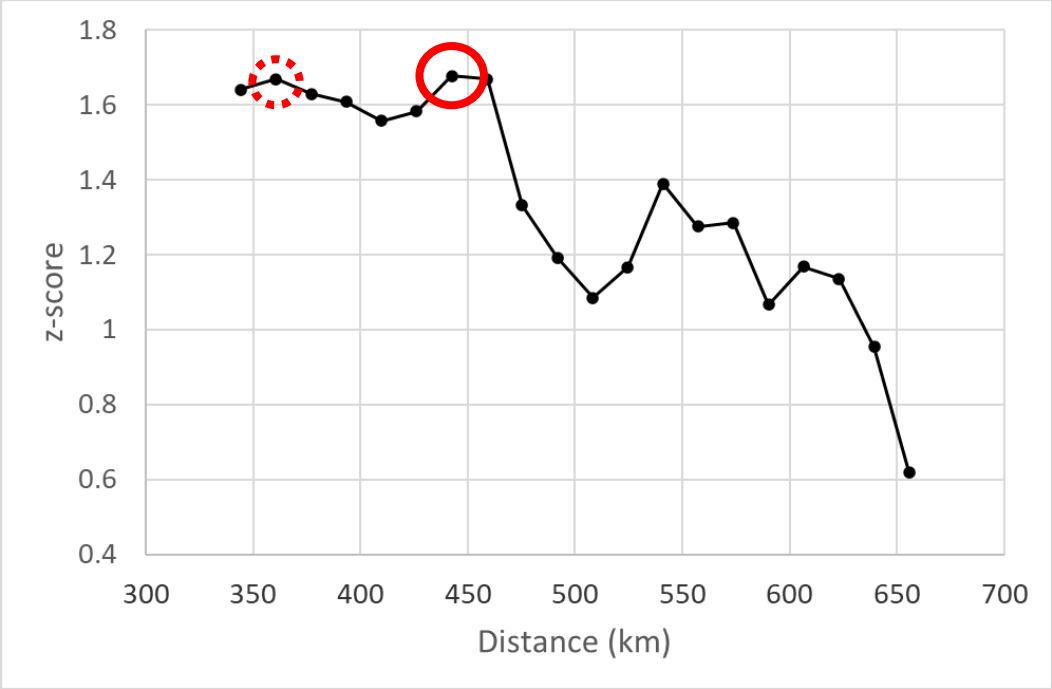

Figure 2.5 Results of Incremental Spatial Autocorrelation of *Varroa destructor* abundance in 2020. The default start distance was 344.3 km increasing by 16.4 km. The first z-score identified in the dashed circle was 360.6 km with the maximum z-score identified in the solid circle being 442.6 km.

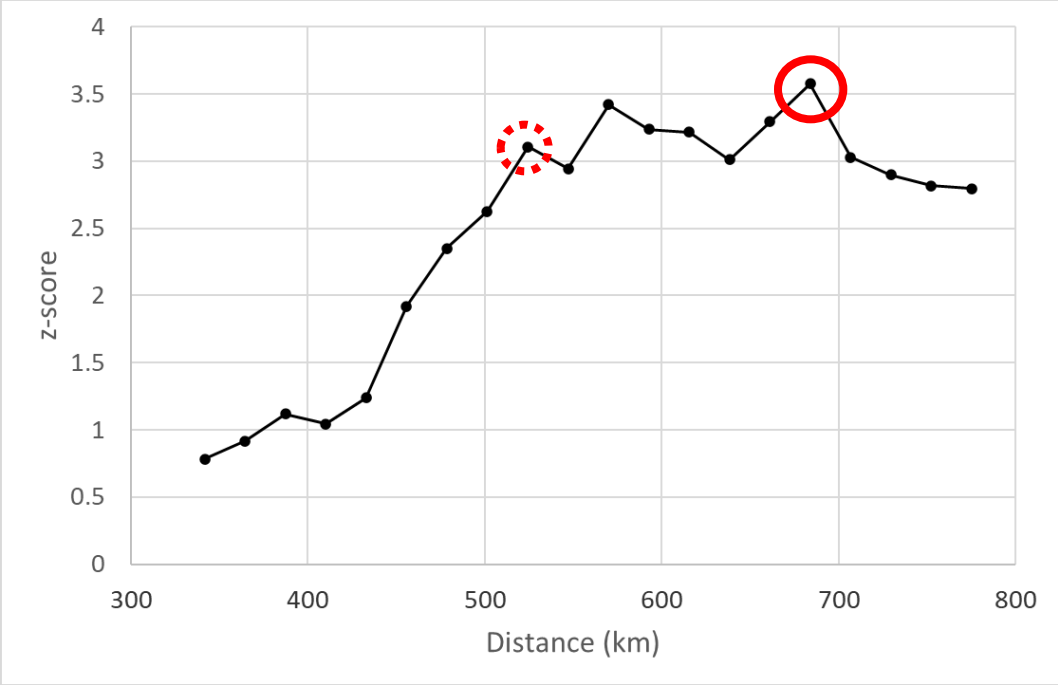

Figure 2.6 Results of Incremental Spatial Autocorrelation of *Varroa destructor* abundance in September of 2017. The default start distance was 341.8 km increasing by 22.8 km. The first z-score identified in the dashed circle was 524.1 km with the maximum z-score identified in the solid circle being 683.7 km.

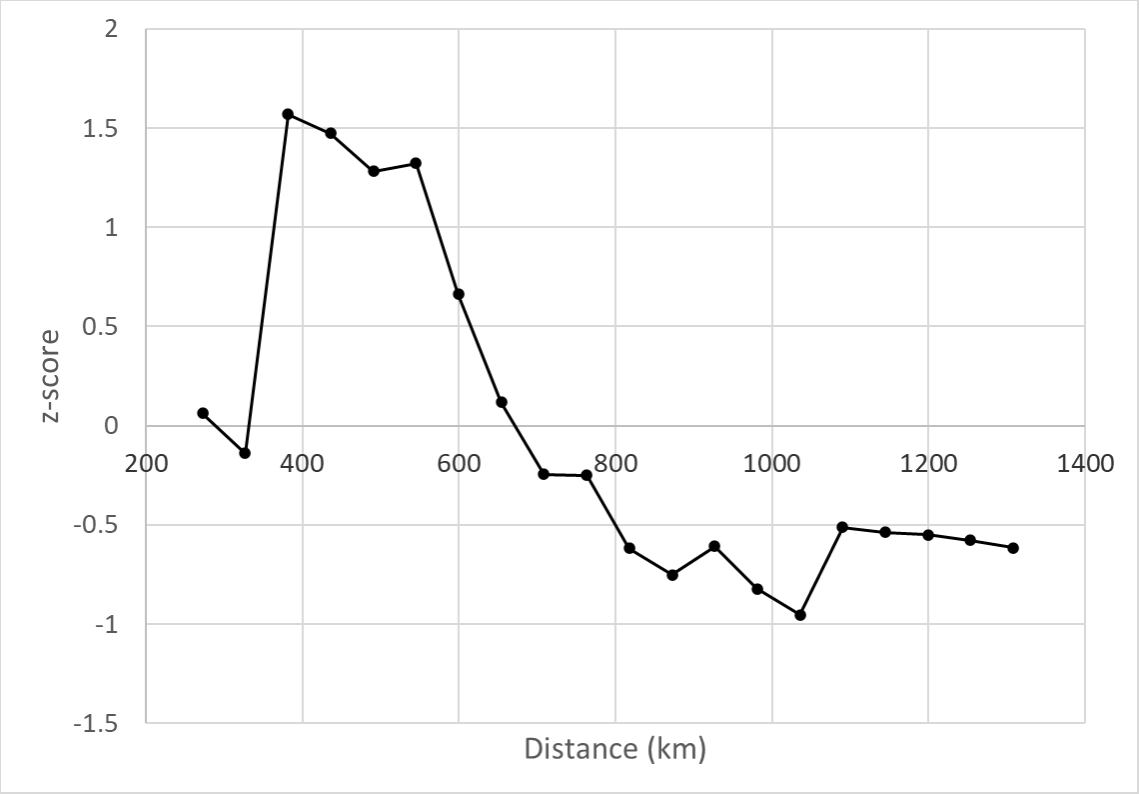

Figure 2.7 Results of Incremental Spatial Autocorrelation of *Varroa destructor* abundance in September of 2019. The default start distance was 272.6 km increasing by 54.5 km. Neither a first z-score peak nor a maximum z-score peak was identified.

2.3.3. Local Indicator of Spatial Autocorrelation

In 2017 all points were found to be non-significant. In 2018 32 points were high-high clusters, 343 points were low-low clusters, 22 points were high-low outliers, 36 points were low-high outliers, and all other points were non-significant (Figure 2.8). In 2020 and September of 2017 all points were found to be non-significant.

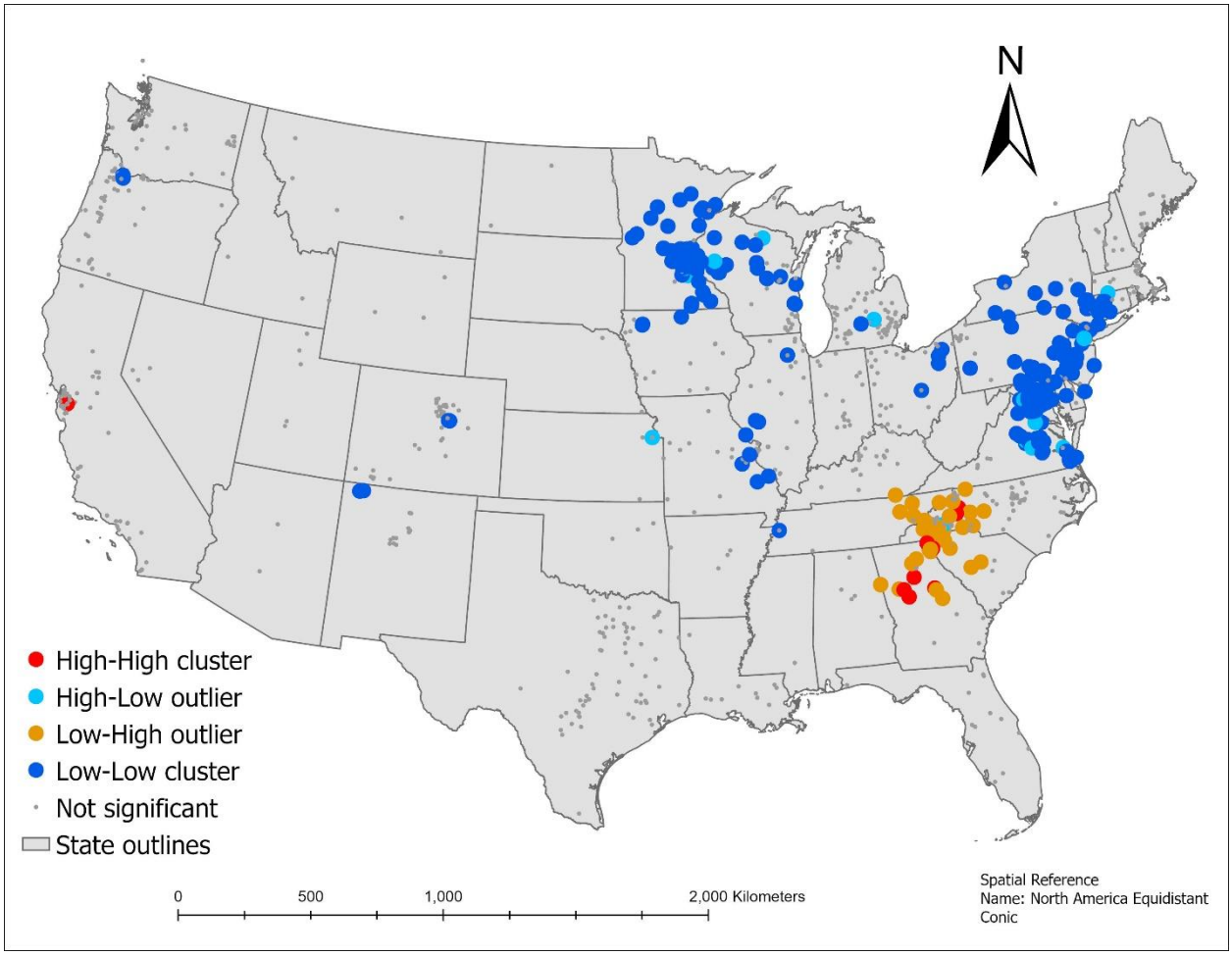

Figure 2.8 Results of the local Moran's *I* of *Varroa destructor* abundance in2018. Red dots represent high-high clusters of *V. destructor*, blue dots represent low-low clusters of *V. destructor*, light blue dots represent high-low outliers of *V. destructor*, orange dots represent low-high outliers of *V. destructor*, and grey points non-significant points of *V. destructor*.

2.3.4 Optimized Outlier Analysis

In 2017 1,171 apiary locations were submitted to MiteCheck with zero bad records included, resulting in 1,171 input features. Twenty-two location outliers were identified and removed resulting in 1,155 final input features. The *Incremental spatial autocorrelation* portion of the *optimized outlier analysis* tool failed to identify a z-score peak, and thus the average distance among 30 neighbors was 176.4 km. In 2017 all points were found to be non-significant.

In 2018 1,527 apiary locations were submitted to MiteCheck with 21 bad records included, resulting in 1,506 input features. Two location outliers were identified and removed resulting in 1,504 final input features. The *Incremental spatial autocorrelation* portion of the *optimized outlier analysis* tool identified a z-score peak at 350.5 km. In 2018 50 points were high-high clusters, 469 were low-low clusters, 45 points were high-low outliers, 115 points were low-high outliers, and all other points were non-significant (Figure 2.9).

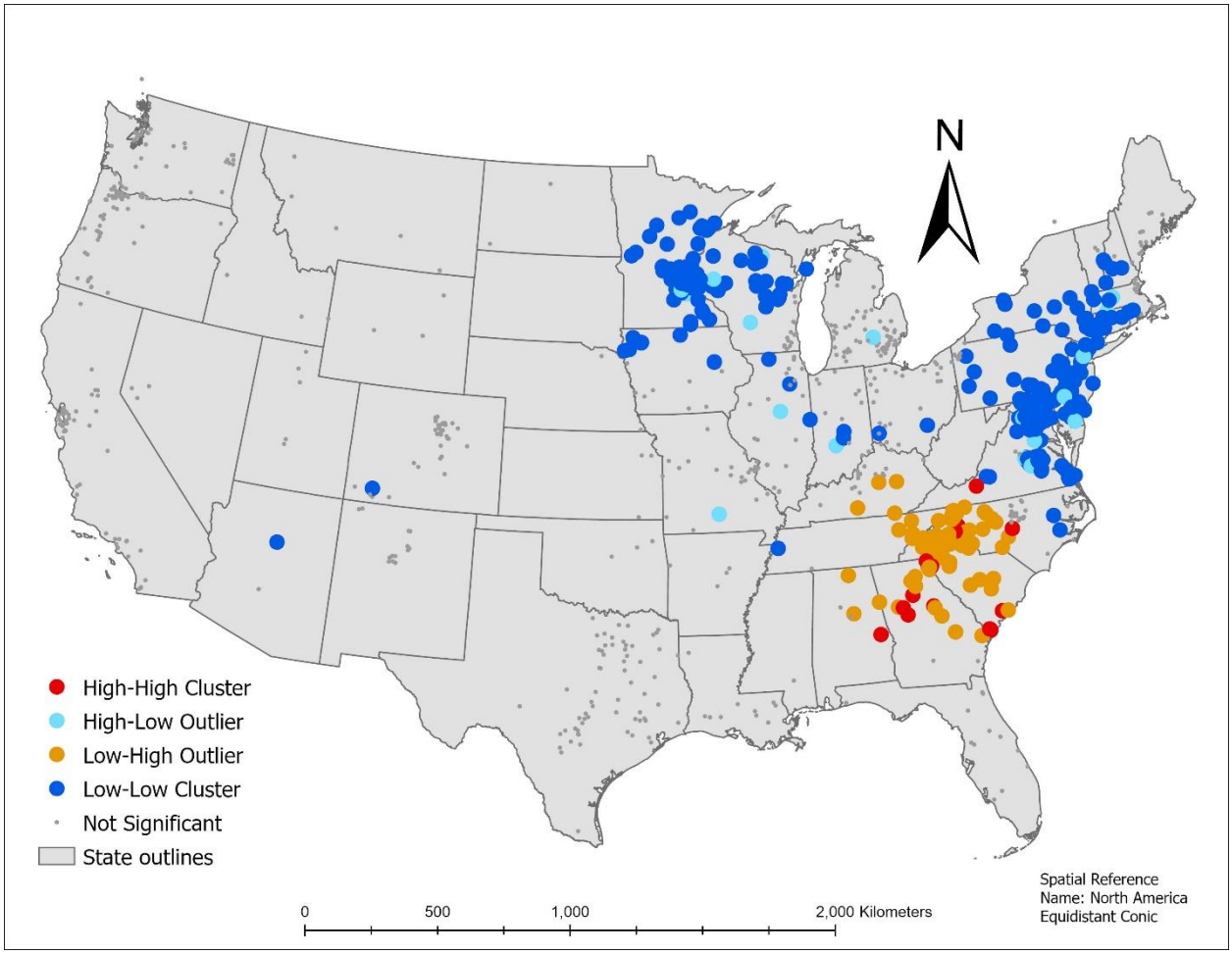

Figure 2.9 Results of the optimized outlier analysis of *Varroa destructor* abundance in 2018. Red dots represent high-high clusters of *V. destructor*, blue dots represent low-low clusters of *V. destructor*, light blue dots represent high-low outliers of *V. destructor*, orange dots represent low-high outliers of *V. destructor*, and grey points non-significant points of *V. destructor*.

In 2019 1,807 apiary locations were submitted to MiteCheck with 708 bad records included, resulting in 1,099 input features. Three location outliers were identified and removed resulting in 1,096 final input features. The *Incremental spatial autocorrelation* portion of the *optimized outlier analysis* tool failed to identify a z-score peak, and thus the average distance among 30 neighbors was 172.6 km. In 2019 18 points were high-high clusters, 11 points were low-low clusters, 2 points were high-low outliers, 83 points were low-high outliers, and all other points were non-significant (Figure 2.10).

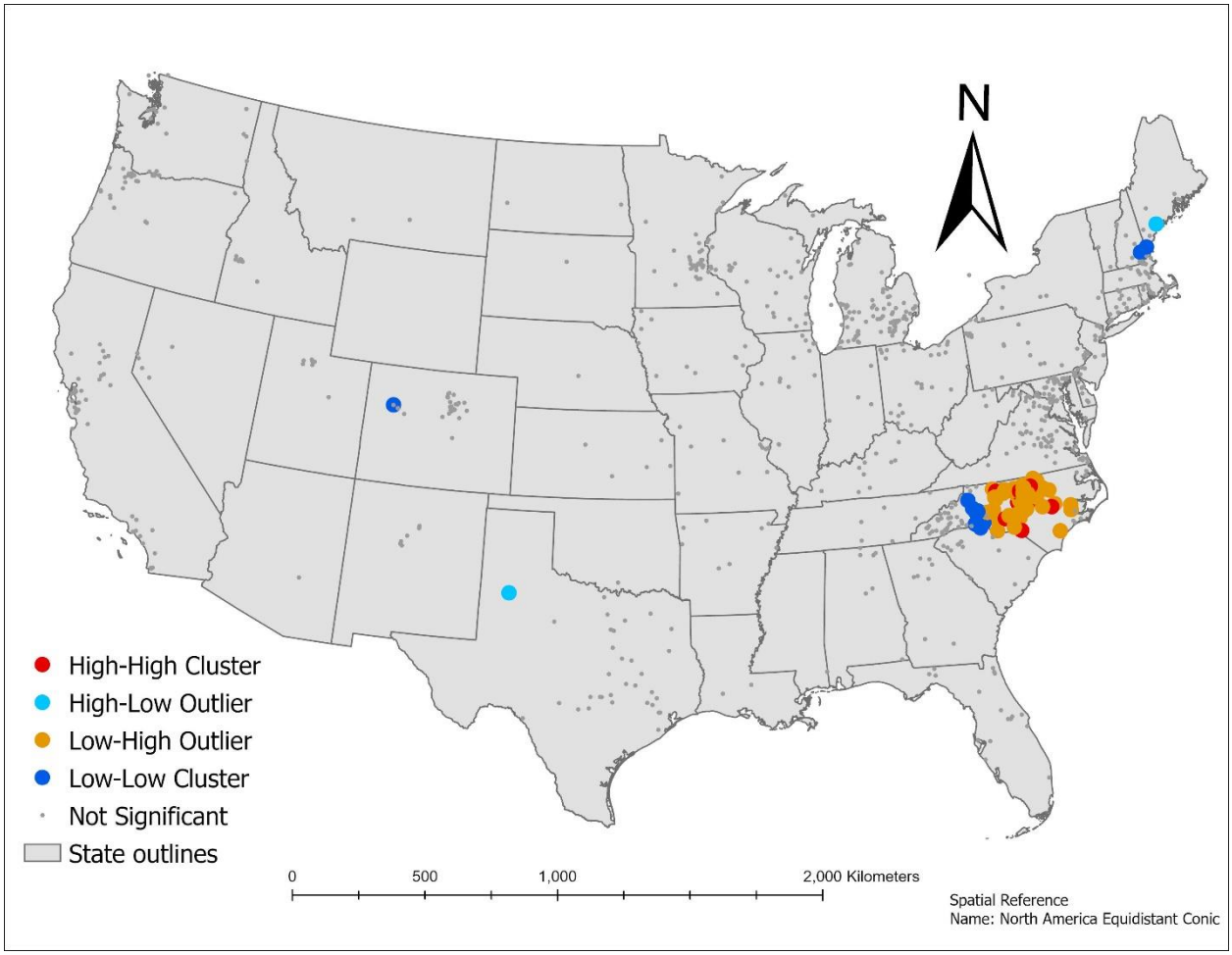

Figure 2.10 Results of the optimized outlier analysis of *Varroa destructor* abundance in 2019. Red dots represent high-high clusters of *V. destructor*, blue dots represent low-low clusters of *V. destructor*, light blue dots represent high-low outliers of *V. destructor*, orange dots represent low-high outliers of *V. destructor*, and grey points non-significant points of *V. destructor*.

In 2020 1,363 apiary locations were submitted to MiteCheck with zero bad records resulting in 1, 363 input features. Twenty-seven location outliers were identified and removed resulting in 1,336 final input features. The *Incremental spatial autocorrelation* portion of the *optimized outlier analysis* tool identified a z-score peak at 184.5 km. In 2020 0 points were high-high clusters, 187 points were low-low clusters, 51 points were high-low outliers, 0 points were low-high outliers, and all other points were non-significant (Figure 2.11).

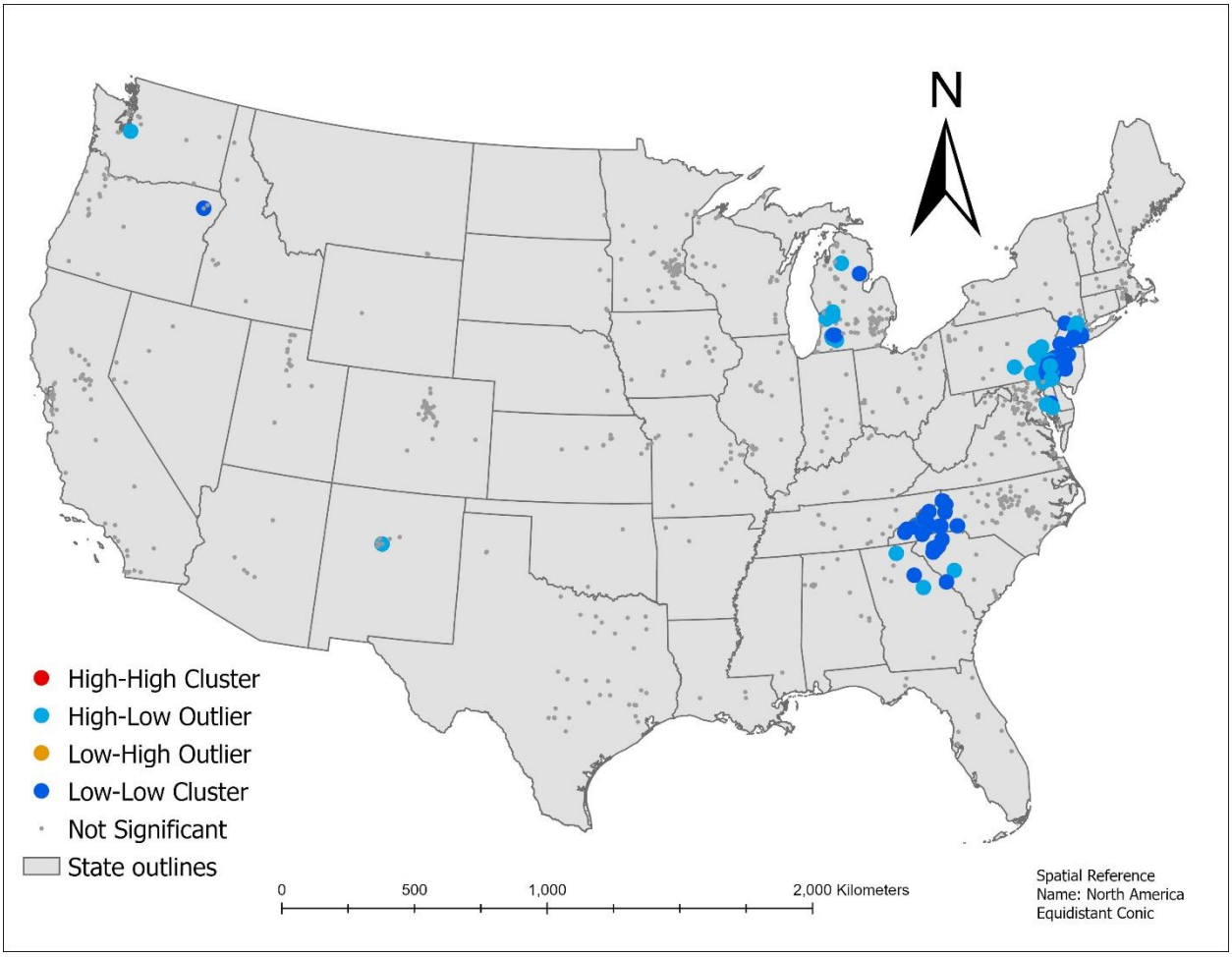

Figure 2.11 Results of the optimized outlier analysis of *Varroa destructor* abundance in 2020. Red dots represent high-high clusters of *V. destructor*, blue dots represent low-low clusters of *V. destructor*, light blue dots represent high-low outliers of *V. destructor*, orange dots represent low-high outliers of *V. destructor*, and grey points non-significant points of *V. destructor*.

In September of 2017 952 apiary locations were submitted to MiteCheck with zero bad records resulting in 952 input features. Twenty-one location outliers were identified and removed resulting in 931 final input features. The *Incremental spatial autocorrelation* portion of the *optimized outlier analysis* tool identified a z-score peak at 177 km. In September of 2017 all points were non-significant.

In September of 2019 739 apiary locations were submitted to MiteCheck with 200 bad records resulting in 539 input features. Four location outliers were identified and removed resulting in 535 final input features. In September of 2019 4 points were high-high clusters, 16 points were low-low clusters, 4 points were high-low outliers, 10 points were low-high outliers, and all other points were non-significant (Figure 2.12).

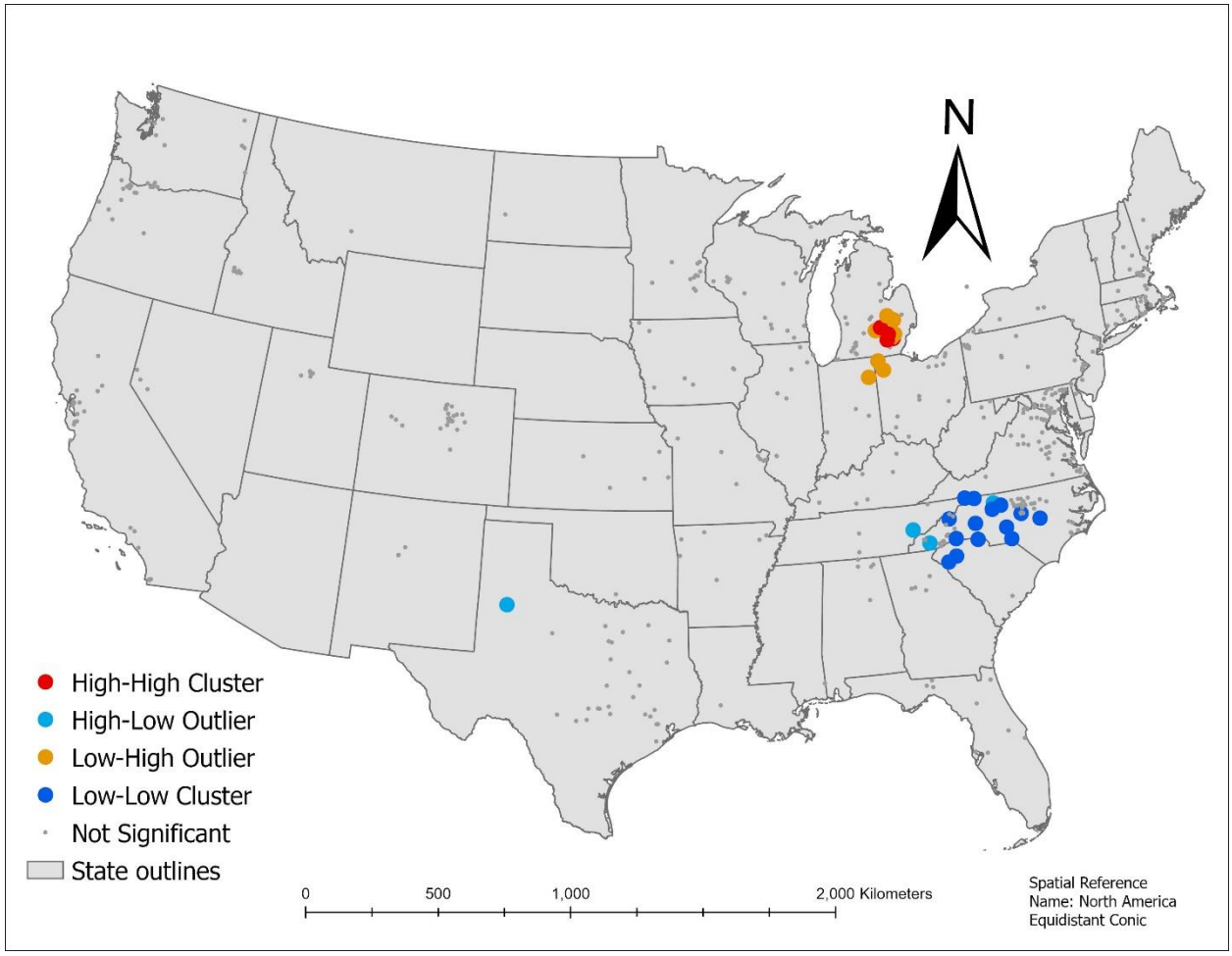

Figure 2.12 Results of the optimized outlier analysis of *Varroa destructor* abundance in September of 2019. Red dots represent high-high clusters of *V. destructor*, blue dots represent low-low clusters of *V. destructor*, light blue dots represent high-low outliers of *V. destructor*, orange dots represent low-high outliers of *V. destructor*, and grey points non-significant points of *V. destructor*.

2.4 Discussion

This research investigated whether *V. destructor* exhibited patterns of spatial clustering in the United States from 2017 to 2020 and whether the inclusion of locational outlier removal and calculating the average nearest neighbor when a z-score peak could not be identified in optimal outlier analysis. I hypothesized that *V. destructor* was spatially autocorrelated and that the optimized outlier analysis would increase the number of high-high and low-low clusters respectively.

2.4.1 Global Moran's I

In subdivisions of data resulting in a statistically significant positive Moran's index value abundance of *V. destructor* was spatially autocorrelated with beekeepers who are close to one another having similar *V. destructor* infestation levels. Subdivisions of data that had larger Moran's index values had higher levels of SA. Thus, the level of SA grew from 2017 to 2019 but fell in 2020. This does not indicate that *V. destructor* abundance declined, rather that the similarity of *V. destructor* abundance across space declined in 2020. The increase in SA of *V. destructor* abundance from 2017 to 2019 is likely the result of similar environmental conditions paired with regional beekeeping practices. Environmental conditions and beekeeper practices that are similar over large areas will drive *V. destructor* abundance to be similar over larger areas, and thus, increase the Moran's index, however, when environmental conditions and beekeeper practices are similar over small areas the abundance of *V. destructor* will be similar over smaller areas, driving the Moran's index down.

In 2017 when the annual Moran's index is compared with the Moran's index of September the Moran's index increased. This increase indicates that the level of SA in *V. destructor* abundance increased. This increase is likely because the surveys submitted in September were temporally closer, and thus, the *V. destructor* infestation levels were more similar. However, when the annual Moran's index is compared to the Moran's index of September in 2018 and 2019 the Moran's index declined. Although surveys submitted in September may be temporally similar, they may not be spatially similar. If spatial closeness or similarity is not present the likelihood of similarity in *V. destructor* abundance declines, and thus, the Moran's index declines.

2.4.2 Manual calculation of neighborhood size and local Moran's I

When the appropriate neighborhood size was manually calculated using the *Incremental spatial autocorrelation* tool z-score peaks indicated the distance at which SA was largest. Z-score peaks were identified in 2017, 2018, 2020, and September of 2017, indicating that an appropriate neighborhood size could be applied to the local Moran's *I* statistic. Alternatively, when a z-score peak was not identified (2019, September of 2019) no appropriate neighborhood size was identified. This is likely the result of multiple spatial processes impacting *V. destructor* abundance, each of which operate at differing scales (ESRI 2022). In this case, environmental conditions and beekeeping practices may be operating at different scales. Additionally, the presence of SA at the global level in 2019 and September of 2019, but the lack of a z-score peak may indicate that when the study area is fragmented into neighborhoods, thus reducing the number of neighbors per feature, this may reduce SA as a result of less features. The inclusion of more features may artificially inflate the SA z-score and *p*-value.

When the local Moran's *I* was calculated using the appropriate neighborhood size, 2018 was the only time period that indicated significant SA. The lack of local SA in 2017, 2019, 2020, and September of 2017 indicates that *V. destructor* abundance was not spatially autocorrelated at the local level. This is likely because when each feature is compared to the local mean there is no significant difference.

In 2018 the presence of local SA indicates that significant differences are present within features of a given neighborhood. Where low-low clusters were present the abundance of *V. destructor* was significantly similar to a low local mean, and conversely, where high-high clusters were present the abundance of *V. destructor* was significantly similar to a high the local mean. Where low-high outliers were present the abundance of *V. destructor* was significantly

lower than the local mean, and conversely where high-low outliers were present *V. destructor* abundance was significantly higher than the local mean.

2.4.3 Optimized outlier analysis

When optimized outlier analysis was applied to time periods with a significantly positive global Moran's index value the number of high-high and low-low clusters increased compared to the manually calculated *Incremental spatial autocorrelation* and local Moran's *I*. In 2017 no local clusters were identified, indicating that *V. destructor* abundance was not significantly similar or different from the local mean. In 2018 a z-score peak was identified at 350.5 km, indicating that *V. destructor* abundance was most spatially autocorrelated at 350.5 km. In 2018 the number of clusters identified rose by 144 apiaries when optimized outlier analysis was applied. Additionally, the neighborhood size rose by 22 km. This indicates that the inclusion of locational outlier removal increased the number of clusters identified. In 2019 a z-score peak was not identified and the average distance to 30 neighbors was used as the appropriate neighborhood size. Additionally, the number of clusters identified rose by 29 apiaries and the neighborhood size rose by 172.6 km as no z-score peak was found in the manual calculation. This indicates that the inclusion of locational outlier removal and distance to 30 neighbors when no z-score peak was identified increased the number of clusters and neighborhood size. In 2020 a z-score peak was found at 184.5 km and the number of clusters rose by 187 apiaries. This again indicated that the inclusion of location outliers decreased the neighborhood size and increased the number of clusters as a result of locational outlier removal. In September of 2017 a z-score peak was identified at 177 km, however, no local SA was identified, indicating that *V. destructor* abundance was not significantly close or distant from the local mean. In September of 2019 no z-score peak was identified and the average distance to 30 neighbors was 265.3 km, indicating that

V. destructor abundance was not significant at increasing neighborhood sizes. Additionally, the number of clusters identified rose by 20 when compared with the manual calculation of neighborhood size and local Moran's *I*. This indicates that the inclusion of location outlier removal and the use of the average distance to 30 neighbors when a z-score was not identified increased the detection of clusters.

2.4.4 Significance for geospatial research

The overall increase in the number of clusters identified when using optimized outlier analysis is significant because the inclusion of locational outlier removal and using the average distance to 30 neighbors when a z-score peak is not identified may artificially inflate cluster detection. Locational outlier removal often decreases the neighborhood detection start distance and thus often lowers the appropriate neighborhood size. When neighborhood sizes are smaller, the likelihood of a feature being similar to the local mean increases due to Tobler's first law of geography which states that near features are more similar than more distant features (Tobler 1965). Locational outlier removal is problematic because although features may be locational outliers, they may still represent the spatial scale of the sample, particularly among large datasets that are spatial spread farther apart.

Furthermore, the calculation of the average distance to 30 neighbors when a z-score peak often reduces the neighborhood size and artificially inflates the detection of clusters. When neighborhood size was manually calculated using the *Incremental spatial autocorrelation* tool and no z-score peak was identified the time period was excluded from further analysis and calculation of the local Moran's *I* because an appropriate neighborhood size was not identified. The shift in calculating the average distance to 30 neighbors in optimized outlier analysis is

problematic because the average distance to 30 neighbors may not represent an appropriate neighborhood size as SA may not be most prominent at the distance.

When using geospatial methods to determine the presence of SA, researchers should be aware of these pitfalls. Manual calculation of neighborhood distance using the *Incremental spatial autocorrelation* tool should be completed and compared to the results of the optimized outlier analysis. The manual calculation of the local Moran's *I* should also be completed and compared to the optimized outlier analysis to determine spatial accuracy. In this context the results of the optimized outlier analysis were most similar to manual calculations in 2018, and thus, are likely accurate. However, when the results of optimized outlier analysis were not similar to the results of manual calculations in all other time periods, the results may be artificially inflated.

2.4.5 Significance for beekeepers

These results are also significant for beekeepers because the presence of SA at the global level indicates that *V. destructor* abundance is on average clustered. Thus, beekeepers should be aware that the abundance of *V. destructor* in neighboring apiaries may impact the level of *V. destructor* abundance within their apiary. Additionally, the presence of local SA in 2018 indicates that apiaries may be present within high-high clusters, and thus the level of *V. destructor* monitoring and treatment may need to be increased. The current survey scheme is to survey ten percent of their colonies once per month from April to October, and before and after treatment is applied (Cornell Cals 2020). Additionally, the current *V. destructor* treatment threshold recommendation is 2 mites per 100 bees in the spring and 3 mites per 100 bees in the fall (Cornell Cals 2020). From these results, the recommendation that beekeepers in the United States should monitor ten percent of their colonies once per month from April to October is

supported, particularly for beekeepers within the high *V. destructor* cluster of the southeast. A close monitoring scheme will allow beekeepers to be alerted earlier in the infestation process and slow the growth of *V. destructor* populations by applying treatment sooner (Delaplane et al. 2005).

2.4.6 Error propagation

Error may have also propagated throughout this analysis because of the citizen science dataset used. Beekeepers were responsible for accurately surveying for *V. destructor* with the method of their choice and reporting to the MiteCheck application, however, the accuracy of these surveys cannot be confirmed, and novel beekeepers may survey incorrectly or misinterpret *V. destructor* survey results. These errors in survey methodology or interpretation may have propagated throughout this analysis because the direct, uncorrected value of *V. destructor* infestation reported by beekeepers was used. If these values were invalid in any way, they could invalidate the Moran's *I* index, and by extension, the significance of spatial clustering. However, the MiteCheck dataset represents the largest and most robust national dataset for *V. destructor* infestation levels in the United States and its use is recommended despite the possibility of input error.

Error may have also propagated throughout this analysis when multiple surveys were completed in the same geographic coordinates within the same month or year and the mean infestation levels were calculated to produce a single *V. destructor* infestation level. This may have skewed results when multiple surveys were completed in the same year *V. destructor* infestation levels peak in the fall as colonies begin to rear more brood before the winter dearth season (Arechavaleta-Velasco and Guzmen-Novoa 2001; Harris et al. 2003). If an apiary completed multiple *V. destructor* surveys in the fall the average *V. destructor* infestation level

would be higher than those apiaries around it that completed surveys in the spring and summer. However, the average infestation level was calculated once in 2017, twice in 2020, and thus the error that may have been introduced from this method was minimal.

2.4.7 Limitations

Limitations of this research include the number of beekeepers participating and the spatial spread of beekeepers from year to year. Although thousands of beekeepers submit their data to MiteCheck many hundreds of thousands of beekeepers do not. The results indicated here may be biased by the relatively small subset of beekeepers that submit to MiteCheck. Additionally, beekeepers may not submit data regularly, which reduces the temporal resolution and the power for statistical accuracy. The irregularity of submissions may also affect the spatial resolution. In some years beekeepers that are near one another may submit their data, while in other years beekeepers that are farther apart may submit their data. This would skew the results of spatial statistics because the likelihood that SA among *V. destructor* abundance increases when apiaries are on average closer together.

Additionally, subdividing the MiteCheck dataset into years may introduce bias. This is because surveys submitted in September-October, when *V. destructor* abundance is highest, may be compared to surveys submitted in February-March, when *V. destructor* abundance is lower. Future research should consider temporal similarity as well as spatial similarity as *V. destructor* abundance is most likely so be similar when data are submitted close in space and in time.

2.4.8 Future research

Further research is needed to elucidate the driving factors of *V. destructor* infestation high and low clusters. Prior research has shown that effective beekeeper management strategies better explain the clustering of *V. destructor* infestation levels than geographic location and

climate (Giacobino et al. 2016), however, climate may continue to drive *V. destructor* infestation levels with high clusters located in more temperate zones, which have longer growing seasons and *V. destructor* has longer access to brood, which it requires for its reproductive cycle (Arechavaleta-Velasco and Guzmen-Novoa 2001; Harris et al. 2003). The regular detection of high clusters in the southeast and west indicates that warmer climates may drive *V. destructor* clustering patterns, however, the high degree of outliers within high-high clusters may be explained by effective beekeeper management strategies.

2.5 Conclusion

Increased rates of honey bee colony loss have been recorded in the United States since 2010 and is significant because honey bees provide billions of dollars in economic value and benefit one third of all human diet. *Varroa destructor* has been identified has a significant driver of honey bee colony loss and been shown to be spatially clustered in Argentina and New Zealand, however, no prior investigation has identified spatial clustering of *V. destructor* in the United States. By obtaining the MiteCheck dataset and applying the global and local Moran's *I* statistic we showed that *V. destructor* infestation levels were significantly spatially clustered at the global level in 2017, 2018, 2019, 2020, and in September of 2017 and September of 2019, and when a LISA was applied high clusters of *V. destructor* infestation were present in the southeast in 2018, while low clusters of *V. destructor* infestation were present in the northeast and in the upper Midwest. Additionally, the application of optimized outlier analysis artificially inflated the detection of clusters through the inclusion of locational outlier removal and calculation of the average distance to 30 neighbors when a z-score peak was not identified. Based on these results it is recommended that beekeepers that are located within high clusters of *V. destructor* monitor and manage for *V. destructor* once per month from April to October.

2.6 References

Ali, H., A.S. Alqarni, J. Iqbal, A.A. Owayss, H.S. Raweh, and B.H. Smith. 2019. "Effect of Season and Behavioral Activity on the Hypopharyngeal Glands of Three Honey Bee *Apis mellifera* L. Races under Stressful Climatic Conditions of Central Saudi Arabia." *Journal of Hymenoptera Research* 68: 85–101. DOI: https://doi.org/10.3897/jhr.68.29678.

Anselin, L. 1995. "Local Indicators of Spatial Association-LISA." *Geographical Analysis* 27 (2): 93–115. DOI: https://doi.org/10.1111/j.1538-4632.1995.tb00338.x.

Arechavaleta-Velasco, M.E., and E. Guzmen-Novoa. 2001. "Relative Effect of Four Characteristics That Restrainthe Population Growth of the Mite *Varroa Destructor* in Honey Bee (*Apis mellifera*) Colonies." *Apidologie* 32(2): 157–74. DOI: https://doi.org/10.1051/apido:2001121.

Azil, A.H., D. Bruce, and C.R. Williams. 2014. "Determining the Spatial Autocorrelation of Dengue Vector Populations: Influences of Mosquito Sampling Method, Covariables, and Vector Control." *Journal of Vector Ecology* 39 (1): 153–163. DOI: https://doi.org/10.1111/j.1948-7134.2014.12082.x.

Ball, B. V., and M. F. Allen. 1988. "The Prevalence of Pathogens in Honey Bee (*Apis mellifera*) Colonies Infested with the Parasitic Mite *Varroa Jacobsoni*." *Annals of Applied Biology* 113 (2): 237–244. DOI: https://doi.org/10.1111/j.1744-7348.1988.tb03300.x.

Beyer, M., J. Junk, M. Eickermann, A. Clermont, F. Kraus, C. Georges, A. Reichart, and L. Hoffmann. 2018. "Winter Honey Bee Colony Losses, *Varroa destructor* Control Strategies, and the Role of Weather Conditions: Results from a Survey among Beekeepers." *Research in Veterinary Science* 118: 52–60. DOI: https://doi.org/10.1016/j.rvsc.2018.01.012.

Bone, C., M.A. Wulder, J.C. White, C. Robertson, and T.A. Nelson. 2013. "A GIS-Based Risk Rating of Forest Insect Outbreaks Using Aerial Overview Surveys and the Local Moran's I Statistic." *Applied Geography* 40: 161–170. DOI: https://doi.org/10.1016/j.apgeog.2013.02.011.

Carreck, N.L., B.V. Ball, and S.J. Martin. 2010. "Honey Bee Colony Collapse and Changes in Viral Prevalence Associated with *Varroa destructor*." *Journal of Apicultural Research* 49 (1): 93–94. DOI: https://doi.org/10.3896/IBRA.1.49.1.13.

Chopra, S.S., B.R. Bakshi, and V. Khanna. 2015. "Economic Dependence of U.S. Industrial Sectors on Animal-Mediated Pollination Service." *Environmental Science & Technology* 49 (24): 14441–14451. DOI: https://doi.org/10.1021/acs.est.5b03788.

Cocu, N., R. Harrington, M. Hulle, and M.D.A. Rounsevell. 2005. "Spatial Autocorrelation as a Tool for Identifying the Geographical Patterns of Aphid Annual Abundance." *Agricultural and Forest Entomology* 7 (1): 31–43. DOI: https://doi.org/10.1111/j.1461-9555.2005.00245.x.

Conte, Y. Le, and M. Navajas. 2008 “Climate Change: Impact on Honey Bee Populations and Diseases.” *Revue scientifique et technique* 27(2): 499-510.

Conte, Y. Le, M. Ellis, and W. Ritter. 2010. “Varroa mites and Honey Bee Health: Can Varroa Explain Part of the Colony Losses?” *Apidologie* 41 (3): 353–363. DOI: https://doi.org/10.1051/apido/2010017.

Cornell Cals. 2020. “Integrated Pest Management (IPM) for Varroa Mite control.” https://pollinator.cals.cornell.edu/sites/pollinator.cals.cornell.edu/files/shared/documents/2020%20IPM%20for%20Varroa%20Mite%20Control.pdf. (accessed March 3, 2022)

De Guzman, L.I., T.E. Rinderer & J.A. Stelzer. 1997. “DNA evidence of the origin of *Varroa jacobsoni* Oudemans in the Americas.” *Biochemical Genetics* 35: 327–335. DOI: https://doi.org/10.1023/A:1021821821728.

Delaplane, KA., J.A. Berry, J.A. Skinner, J.P. Parkman & W.M. Hood. 2005. “Integrated pest management against *Varroa destructor* reduces colony mite levels and delays treatment threshold.” *Journal of Apicultural Research* 44 (4): 157-162. DOI: https://doi.org/10.1080/00218839.2005.11101171.

Delfinado, M. 1963. “Mites of the honeybee in South East Asia.” *Journal of Apicultural Research* 2: 113–114. https://doi.org/10.1080/00218839.1963.11100070.

de Miranda, J.R., G. Corodoni, G. Budge. 2010. “The acute bee paralysis virus-kashmire bee virus-israeli acute paralysis virus complex*.” Journal of Invertebrate Pathology* 103: S30-S47. DOI: https://doi.org/10.1016/j.jip.2009.06.014.

Dooremalen, C. van, L. Gerritsen, B. Cornelissen, J.J.M. van der Steen, F. van Langevelde, and T. Blacquière. 2012. “Winter Survival of Individual Honey Bees and Honey Bee Colonies Depends on Level of *Varroa destructor* Infestation.” Edited by Mark F. Feldlaufer. *PLoS ONE* 7 (4): e36285. DOI: https://doi.org/10.1371/journal.pone.0036285.

ESRI. 2022. “Incremental Spatial Autocorrelation (Spatial Statistics).” https://pro.arcgis.com/en/pro-app/2.8/tool-reference/spatial-statistics/incremental-spatial-autocorrelation.htm. (accessed March 3, 2022)

Fries, I., P. Rosenkranz. 1996. “Number of reproductive cycles of *Varroa jacobsoni* in honey-bee (*Apis mellifera*) colonies. *Experimental and Applied Acarology* 20: 103–112. https://doi.org/10.1007/BF00051156.

Fries, I., S. Camazine & J. Sneyd. 1994. “Population Dynamics of *Varroa Jacobsoni*: A Model and a Review.” *Bee World* 75(1): 5-28. DOI: https://doi.org/10.1080/0005772X.1994.11099190.

Gallai, N., J.-M. Salles, J. Settele, and B.E. Vaissière. 2009. “Economic Valuation of the Vulnerability of World Agriculture Confronted with Pollinator Decline.” *Ecological Economics* 68 (3): 810–21. DOI: https://doi.org/10.1016/j.ecolecon.2008.06.014.

Giacobino, A., A. Molineri, N. Bulacio Cagnolo, J. Merke, E. Orellano, E. Bertozzi, Germán M. 2016. “Key Management Practices to Prevent High Infestation Levels of *Varroa Destructor* in Honey Bee Colonies at the Beginning of the Honey Yield Season.” *Preventive Veterinary Medicine* 131: 95–102. DOI: https://doi.org/10.1016/j.prevetmed.2016.07.013.

Giacobino, A., A. Molineri, N. Bulacio Cagnolo, J. Merke, E. Orellano, E. Bertozzi, G. Masciángelo. 2015. “Risk Factors Associated with Failures of Varroa Treatments in Honey Bee Colonies without Broodless Period.” *Apidologie* 46(5): 573–582. https://doi.org/10.1007/s13592-015-0347-0.

Giacobino, A., N. Bulacio Cagnolo, J. Merke, E. Orellano, E. Bertozzi, G. Masciangelo, H. Pietronave, C. Salto, and M. Signorini. 2014. “Risk Factors Associated with the Presence of Varroa destructor in Honey Bee Colonies from East-Central Argentina.” Preventive Veterinary Medicine 115 (3–4): 280–87. DOI: https://doi.org/10.1016/j.prevetmed.2014.04.002.

Harris, J. W., J. R. Harbo, J. D. Villa, and R. G. Danka. 2003. “Variable Population Growth of *Varroa destructor* (*Mesostigmata: Varroidae*) in Colonies of Honey Bees (*Hymenoptera: Apidae*) During a 10-Year Period.” *Environmental Entomology* 32(6): 1305–12. DOI: https://doi.org/10.1603/0046-225X-32.6.1305.

Klein, A.M., B.E. Vaissière, J.H. Cane, I. Steffan-Dewenter, S.A. Cunningham, C. Kremen, and T. Tscharntke. 2007. “Importance of Pollinators in Changing Landscapes for World Crops.” *Proceedings of the Royal Society B: Biological Sciences* 274(1608): 303–313. https://doi.org/10.1098/rspb.2006.3721.

Kraus, B., and R. E. Page. 1995. “Population Growth of *Varroa jacobsoni* Oud in Mediterranean Climates of California.” *Apidologie* 26 (2): 149–157. DOI: https://doi.org/10.1051/apido:19950208.

Kulhanek, K., N. Steinhauer, K. Rennich, D.M. Caron, R.R. Sagili, J.S. Pettis, J.D. Ellis, M.E. Wilson, J.T. Wilkes, D.R. Tarpy, R. Rose, K. Lee, J. Rangel & D. vanEngelsdorp. 2017. “A national survey of managed honey bee2015–2016 annual colony losses in the USA.” *Journal of Apicultural Research* 56 (4): 328-340. DOI: https://doi.org/10.1080/00218839.2017.1344496.

Lee, K. V., R. D. Moon, E. C. Burkness, W. D. Hutchison, and M. Spivak. 2010. “Practical Sampling Plans for *Varroa destructor* (*Acari: Varroidae*) in *Apis mellifera* (*Hymenoptera: Apidae*) Colonies and Apiaries.” *Journal of Economic Entomology* 103(4): 1039–50. DOI: https://doi.org/10.1603/EC10037.

Locke, B. 2016. “Natural Varroa Mite-Surviving *Apis mellifera* Honeybee Populations.” *Apidologie* 47(3): 467–82. DOI: https://doi.org/10.1007/s13592-015-0412-8.

Martin, S.J. 2001. “The Role of Varroa and Viral Pathogens in the Collapse of Honeybee Colonies: A Modelling Approach: Collapse of Varroa -Infested Honeybee Colonies.”

Journal of Applied Ecology 38 (5): 1082–93. DOI: https://doi.org/10.1046/j.1365-2664.2001.00662.x.

Martin, S.J., and L.E. Brettell. 2019. "Deformed Wing Virus in Honeybees and Other Insects." *Annual Review of Virology* 6 (1): 49–69. DOI: https://doi.org/10.1146/annurev-virology-092818-015700.

Millar, R.B., and M.J. Anderson. 2004. "Remedies for Pseudoreplication." *Fisheries Research* 70 (2–3): 397–407. DOI: https://doi.org/10.1016/j.fishres.2004.08.016.

MiteCheck. 2021. *Varroa destructor* infestation levels (2015-2021). https://research.beeinformed.org/mitecheck/ (accessed August 12, 2021).

Moran, P.A. P. 1950. "Notes on Continuous Stochastic Phenomena." *Biometrika* 37(1/2): 17–23. DOI: https://doi.org/10.2307/2332142.

Nelson, T.A., and B. Boots. 2008. "Detecting Spatial Hot Spots in Landscape Ecology." *Ecography* 31 (5): 556–66. DOI: https://doi.org/10.1111/j.0906-7590.2008.05548.x.

Oldroyd, B.P. 2007. "What's Killing American Honey Bees?" *PLoS Biology* 5(6): 1195-1199. DOI: https://doi.org/10.1371/journal.pbio.0050168.

Oudemans, A.C. 1904. "On a new genus and species of parasitic acari." *Notes from the Leyden Museum* 24(4): 216-222. DOI: https://repository.naturalis.nl/pub/508650.

Ramsey, S.D., R. Ochoa, G. Bauchan, C. Gulbronson, J.D. Mowery, A. Cohen, D. Lim. 2019. "*Varroa destructor* Feeds Primarily on Honey Bee Fat Body Tissue and Not Hemolymph." *Proceedings of the National Academy of Sciences* 116(5): 1792–1801. DOI: https://doi.org/10.1073/pnas.1818371116.

Ritter, W. 1981. "Varroa Disease of the Honeybee *Apis Mellifera*." *Bee World* 62(4): 141-153. DOI: https://doi.org/10.1080/0005772X.1981.11097838.

Ruttner, F. & V. Maul. 1983. "Experimental analysis of reproductive interspecies: Isolation of *Apis mellifera* L. and *Apis cerana* Fabr." *Apidologie* 14: 309–327. DOI: https://doi.org/10.1051/apido:19830405.

Saiki, T. & I. Okada. 1973. "The present beekeeping in Japan." *Glean Bee Culture* 101: 356–357.

Steinhauer, N.A, K. Rennich, M.E. Wilson, D.M. Caron, E.J. Lengerich, J.S. Pettis, R. Rose. 2014. "A National Survey of Managed Honey Bee 2012–2013 Annual Colony Losses in the USA: Results from the Bee Informed Partnership." *Journal of Apicultural Research* 53 (1): 1–18. DOI: https://doi.org/10.3896/IBRA.1.53.1.01.

Stevenson, M.A., H. Benard, P. Bolger, and R.S. Morris. 2005. "Spatial Epidemiology of the Asian Honey Bee Mite (*Varroa destructor*) in the North Island of New Zealand." *Preventive Veterinary Medicine* 71(3–4): 241–252. DOI: https://doi.org/10.1016/j.prevetmed.2005.07.007.

Sumpter, D. J. T., and S. J. Martin. 2004. “The Dynamics of Virus Epidemics in Varroa -Infested Honey Bee Colonies.” *Journal of Animal Ecology* 73 (1): 51–63. DOI: https://doi.org/10.1111/j.1365-2656.2004.00776.x.

Tautz, J. 2008. The buzz about bees: biology of a super-organism. Springer-Verlag Berlin Heidelberg.

Tobler, W.R. 1965. “Computation of the correspondence of geographical patterns.*” Papers of the Regional Science Association* 15: 131–139. DOI: https://doi.org/10.1007/BF01947869.

Tosi, S., F.J. Démares, S.W. Nicolson, P. Medrzycki, C.W.W. Pirk, and H. Human. 2016. “Effects of a Neonicotinoid Pesticide on Thermoregulation of African Honey Bees (*Apis mellifera scutellata*).” *Journal of Insect Physiology* 93–94: 56–63. DOI: https://doi.org/10.1016/j.jinsphys.2016.08.010.

Traynor, K.S., F. Mondet, J.R. de Miranda, M. Techer, V. Kowallik, M.A.Y. Oddie, P. Chantawannakul, and A. McAfee. 2020. “*Varroa destructor*: A Complex Parasite, Crippling Honey Bees Worldwide.” *Trends in Parasitology* 36 (7): 592–606. DOI: https://doi.org/10.1016/j.pt.2020.04.004.

Traynor, K.S., K. Rennich, E. Forsgren, R. Rose, J. Pettis, G. Kunkel, S. Madella, J. Evans, D. Lopez, and D. vanEngelsdorp. 2016. “Multiyear Survey Targeting Disease Incidence in US Honey Bees.” *Apidologie* 47 (3): 325–347. DOI: https://doi.org/10.1007/s13592-016-0431-0.

vanEngelsdorp, D., J. Hayes, R.M. Underwood, and J. Pettis. 2008. “A Survey of Honey Bee Colony Losses in the U.S., Fall 2007 to Spring 2008.” Edited by Nick Gay. *PLoS ONE* 3 (12): e4071. DOI: https://doi.org/10.1371/journal.pone.0004071.

Vaudo, A.D., J.D. Ellis, G.A. Cambray, and M. Hill. 2012. “The Effects of Land Use on Honey Bee (*Apis mellifera*) Population Density and Colony Strength Parameters in the Eastern Cape, South Africa.” *Journal of Insect Conservation* 16 (4): 601–611. DOI: https://doi.org/10.1007/s10841-011-9445-0.

Chapter 3

Assessing the application of a drone equipped with a thermal sensor for surveying honey bee (*Apis mellifera)* colony health

3.1 Introduction

Precision agriculture is the use of technology to measure temporal and spatial trends to support management decisions in agricultural settings (Pierce and Nowak 1999). Technologies that have been applied include drones equipped with multispectral, thermal, red, green blue, and light detection and ranging (LiDAR) sensors (Daponte et al. 2019). Drones equipped with multispectral sensors have been used to monitor crops by measuring chlorophyll content, leaf water content, ground cover and leaf area index (Stehr 2015). Drones equipped with a thermal sensor have been used to detect water stress in crops because they present higher temperatures, and therefore higher thermal reflectance (Svatos and Trowbridge 2018). Apiculture, or the maintenance of honey bee (*Apis mellifera*) colonies, is a subset of agriculture and the technologies that have been applied in precision agriculture are highly applicable to precision apiculture, including drones equipped with multispectral and thermal sensor (Zacepins et al. 2012). Similar to precision agriculture, precision apiculture specifically measures the temporal and spatial trends of honey bee colonies to support management decisions (Zacepins et al. 2012). Precision apiculture has employed the use of internal colony temperature sensors (Braga et al. 2020) and thermal imagers (Lim et al. 2013; Shaw et al. 2010) to measure the average colony temperature. Specifically, Braga et al. (2020) used average colony temperatures captured by internal temperature sensors in tandem with ambient weather data and colony inspections to train a classification algorithm, which accurately predicted the colony health status with 90%

accuracy. Additionally, Shaw et al. (2010) used external thermal imaging to examine the relationship between average colony temperature and the population of adult bees and found that higher average colony temperatures were positively correlated with the population of adult bees. Specifically, Shaw et al. (2010) completed manual colony inspections, measured the number of complete frames covered by adult bees, captured thermal images of 33 colonies, measured the average colony temperature from the thermal images, and used a t-test to determine the level of correlation between the number of complete frames covered by adult bees and the average colony temperature. Similarly, Lim et al. (2013) used external thermal imaging to investigate the difference in average colony temperature between colonies that survived the winter and those that did not. They found that colonies that survived the winter had a higher average colony temperature of 2-6°C, and again indicated that external thermal imaging can be used to determine the health of a honey bee colony by measuring average colony temperature (Lim et al. 2013). Thus, the application of external thermal imaging in precision apiculture has been successful and the average colony temperature and population of adult bees is significantly positively correlated (Lim et al. 2013; Shaw et al. 2010).

Although other metrics of honey bee colony health including the amount of brood (developing bees) and carbohydrate resources (honey) have been included to predict colony survivorship (Braga et al. 2020) they have not been included in investigations of average colony temperature as measured by external thermal imagers (Lim et al. 2013 and Shaw et al. 2010). The inclusion of other metrics of honey bee colony health like the amount of brood and honey may increase the explanatory power between the average colony temperature and metrics of honey bee colony health from $R^2 = 0.63$ found in Shaw et al. (2010). Other metrics may be analyzed through the application of backward stepwise model building. Other metrics of honey

bee colony health that are measured in manual colony health inspections but have not been included in investigations of average colony health remain significant to overall honey bee colony health. Specifically, higher amounts of adult bees reflect higher levels of honey bee colony health. Higher amounts of brood (developing larvae) reflect higher levels of honey bee colony health. Higher amounts of carbohydrate resources reflect higher levels of honey bee colony health.

Precision apiculture and the accurate measure of honey bee populations are significant because honey bees are an economically significant agricultural livestock that indirectly benefit 35% of all human diet (Klein et al. 2007). Beekeepers anticipate annual colony losses between 8-20%, typically due to reduced floral resources and adverse weather conditions in winter (Kulhanek et al. 2017), however, elevated rates of honey bee colony loss have been documented in the Northern Hemisphere since 2007 (Oldroyd 2007). Most recently in the United States the rate of honey bee colony loss has exceeded 40% in 2020 (Bruckner et al. 2020). Early warning signs of colony loss are identified via close monitoring schemes (Dainat et al. 2012), which involve opening the lids, manually removing frames, and inspecting each frame for the amount of adult bees, brood, and resources including honey and pollen (Delaplane et al. 2013). As a result of the manual dismantling and inspection of the colony, close monitoring schemes are time and labor intensive. Moreover, this process threatens the loss of the queen, which disrupts the reproductive cycle of the colony, and in winter the disruption of the colony structure lowers the colony temperature and can negatively impact the winter survivorship of the colony (Stabentheiner et al. 2002). Thus, non-invasive methods of honey bee colony inspection, which include thermal image capture and measurement of the average colony temperature, may avoid

these negative impacts of invasive colony inspection while still providing early warning signs of honey bee colony loss.

Backward stepwise model building can be used to identify the significance of predictor variables, but it is generally accepted that backward stepwise model building should be used to select the most parsimonious set of predictor variables for a final model (Huberty 1989). Backward stepwise model building allows for variables to be selected from a larger set of predictors and is useful for variance reduction and parsimony (Thompson 1995). Backward stepwise model building works by including all variables of interest, running the model, and removing the variable with the least statistical significance (Efroymson 1960). This process is repeated until all variables are statistically significant.

Therefore, I further investigated non-invasive honey bee colony inspection methods using external thermal imagers and included the amount of adult bees, brood, and honey in our investigation. I hypothesized that the inclusion of the amount of adult bees, brood, honey, and the position of bees, brood, and honey will further elucidate the relationship between honey bee colony health and average colony temperature as shown by statistical significance of variables in a final model. Additionally, due to the current minimal use of drone technology in precision apiculture, despite its widespread applicability in precision agriculture, I also investigated if an external thermal sensor mounted to a drone could accurately measure the average colony temperature and whether the outer and/or inner lid needed to be removed for accurate measurement. I hypothesized that the average colony temperature will most accurately be measured with the inner and outer lid removed, thus allowing beekeepers to remove the lids, capture a thermal image, and estimate honey bee colony health. This will be shown if all variables included are significant with both lids removed. The statistical significance of all

variables with no lids in place is significant because it reduces the time and effort required for colony health surveys.

3.2 Methods

3.2.1 Manual Colony Inspection

This research was completed at the Richland Bee Yard in Auburn, AL, USA. The yard contained 47 honey bee colonies in total; however, 15 colonies were selected for thermal image capture. Each colony was double deep containing two brood chambers. Manual colony inspections of adult bees, brood, honey, and the position of adult bees, brood, and honey were conducted two weeks prior to thermal image sampling. Manual colony surveys were completed by examining each frame within each colony and determining the percent coverage for each variable by using the Liebefeld method (Delaplane et al. 2013). The colonies that were selected for thermal image capture included the five colonies with the highest amount of adult bees, the five colonies with the lowest amount of adult bees, and five colonies with the median amount of adult honey bees (Table 3.1). Proportion of adult bees in the top box, proportion of capped brood in the top box, and the proportion of honey in the top box were calculated by dividing the total number of frames of the respective variable (adult bees/capped brood/honey) in the top box with the total frames of the respective variable in the colony to estimate the position of bees, brood, and honey.

3.2.2 Thermal Image Capture

Three thermal images of each colony were captured including images with the outer and inner lid on, with only the inner lid, and with no lid using a DJI Matrice 200 V2 drone equipped with a Micasense Altum thermal sensor.. For this preliminary test the drone was not flown, but held at a distance of ~1 meter above the colony to maintain compliance with local drone regulations (Figure 3.1).

Figure 3.1 Thermal image capture of a honey bee (*Apis mellifera*) colony from above with inner and outer lids in place. Thermal images were captured with a DJI Matrice 200 V2 drone equipped with a Micasense Altum thermal sensor. The thermal image taken here was from above with the inner and outer lids in place.

Table 3.1 Metrics of honey bee (*Apis mellifera*) colony health by colony. Colony number represents individual colonies and their position in the bee yard. Sides of adult bees represents the number of the sides with adult bees covering them. Sides of brood represents the number of sides with brood covering them. Proportion of adult bees in the top box represents the number of sides of adult bees in the top box divided by the total number of the sides of adult bees. Proportion of brood in the top box represents the number of sides of brood in the top box divided by the total number of sides of brood. Proportion of honey in the top box represents the number of sides of honey in the top box divided by the total number of sides of honey.

Colony Number	Sides of adult bees	Sides of brood	Proportion of adult bees in the top box	Proportion of brood in the top box	Proportion of honey in the top box
1	5.93	2.90	0.68	1.00	0.86
2	5.93	1.85	0.29	0.32	0.90
3	13.00	3.20	0.34	1.00	0.89
4	15.30	2.63	0.35	0.94	0.85
5	3.20	1.95	0.91	1.00	1.00
6	4.20	2.65	0.96	1.00	0.96
7	2.70	1.88	0.90	1.00	0.95
8	3.10	2.95	0.98	1.00	1.00
9	2.93	1.23	0.06	0.00	0.72
10	12.30	5.75	0.56	1.00	0.61
11	6.40	0.68	0.55	1.00	0.62
12	12.90	4.70	0.36	0.43	0.64
13	6.98	2.45	0.92	1.00	0.88
14	14.25	2.50	0.49	1.00	0.59
15	2.88	1.45	0.67	1.00	0.97

3.2.3 Thermal Image Processing

Using ArcGIS Pro 2.8, each image was clipped to include only the area of the colony (Figure 2). Pixel size within each image was resampled to the coarsest resolution captured (0.39 cm by 0.39 cm) to maintain consistent image and pixel size. Temperature values of each pixel were then converted from the default Centikelvin to Celsius (Equation 1). Average temperature was identified by applying zonal statistics.

$$C° = \frac{cK°}{100} - 273.1 \quad (1)$$

3.3.4 Statistical analysis

Backward stepwise model building was applied to the average temperatures obtained from images with no lids, inner lid only, and inner and outer lid respectively, with the global model including the average colony temperature as the response variable, and amount of adult bees as measured in colony frame coverage, amount of capped brood as measured in colony frame coverage, amount of honey as measured in colony frame coverage, proportion of adult bees in the top box, proportion of capped brood in the top box, and proportion of honey in the top box as explanatory variables. Once the global model was completed the least significant variable as measured by the *p*-value was removed. This process was repeated until all variables in the model were statistically significant or confounding. Statistical significance of alpha = 0.1 was used.

3.3 Results

3.3.1 Inner and Outer lid in place

The average temperature of colonies with both the inner lid and outer lid in place was 6.6°C. When backward stepwise model building was applied including all variables, the proportion of adult bees in the top box was only significantly associated with the average colony temperature (*p*-value = 0.09) (Table 3.1). The least significant variable was the proportion of brood in the top box, and thus it was removed (*p*-value = 0.99). The next model included amount of adult bees, amount of brood, proportion of adult bees in the top box, and proportion of honey in the top box. The least significant variable of this model was amount of brood, and thus it was removed (*p*-value = 0.67). The next model included amount of adult bees, proportion of adult bees in the top box, and proportion of honey in the top box. The least significant variable of this model was the amount of adult bees, and thus it was removed (*p*-value = 0.49). The next model included the proportion of adult bees in the top box and the proportion of honey in the top box.

Both variables were significant, and thus the final model was identified (Table 3.2). The final model had an r-squared value of 0.4 and a *p*-value of 0.05.

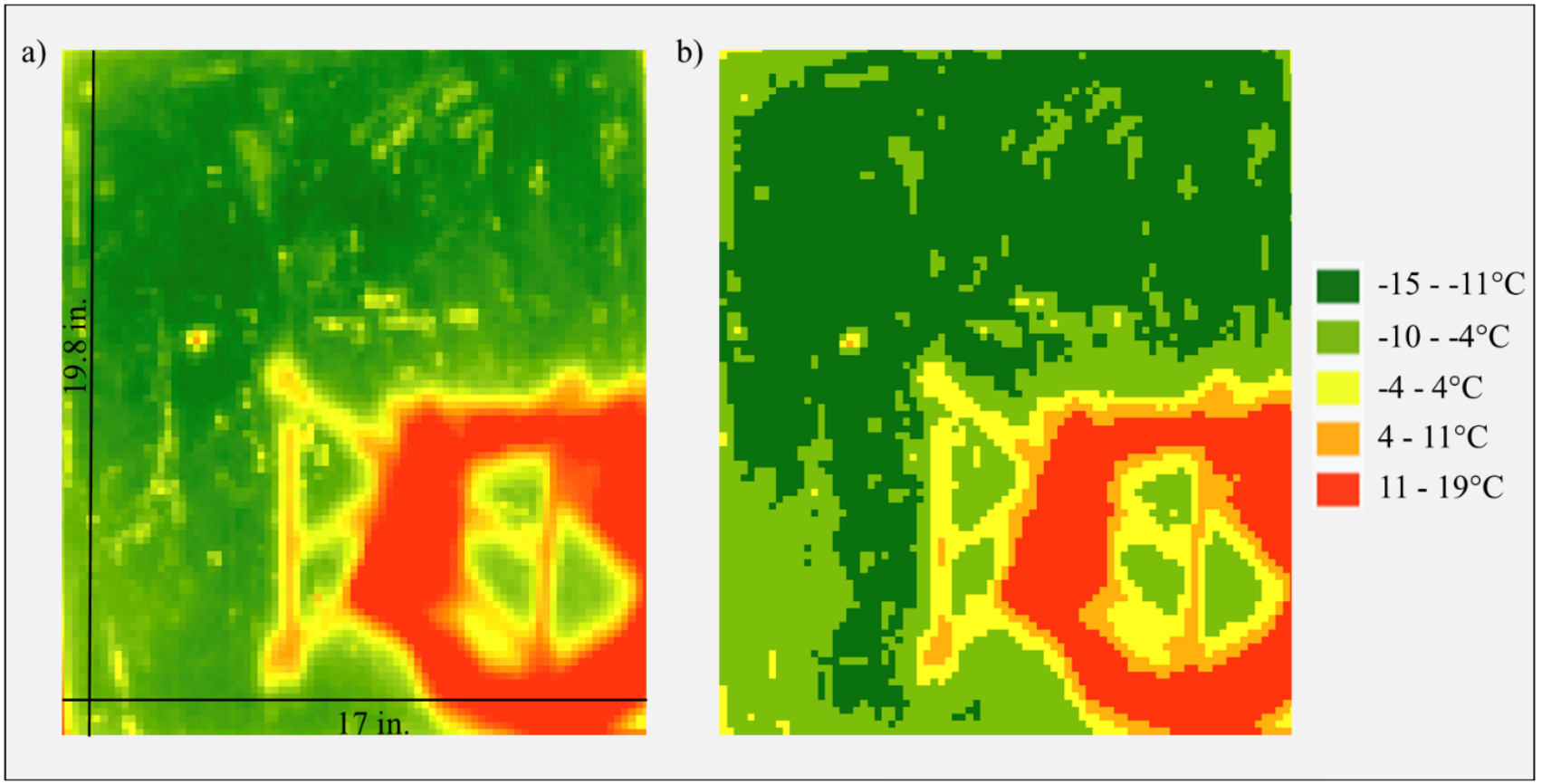

Figure 3.2. Thermal images of honey bee (*Apis mellifera*) colony one with the inner and outer lid in place. Thermal images of colony one with the inner and outer lid in place with the raw image (a), and the transformed image (b). In both images dark green represents 13-17°C, light green represents 17-20°C, yellow represents 20-22°C, orange represents 22-25°C, and red represents 25-30°C. Each colony had standard dimensions and measures 19.8 inches by 17 inches. Each colony had standard dimensions and measures 19.8 inches by 17 inches. The shadow of the drone being held above the colony can be seen in red in both images.

Table 3.2 Inner and outer lid in place global model results. Variable represents all variables included in the model, estimate represents the estimate of effect, standard error represents the 95% confidence interval, and the *p*-value represents the statistical significance with statistically significant values indicate by an asterisk (*).

Variable	Estimate	Standard error	*p* -value
Sides of adult bees	-0.14	0.26	0.61
Sides of brood	0.24	0.63	0.71
Proportion of adult bees in the top box	0.051	0.049	0.33
Proportion of brood in the top box	-0.0001	0.037	0.99
Proportion of honey in the top box	-0.094	0.050	0.09*

Table 3.3 Inner and outer lid in place final model results. Variable represents all variables included in the model, estimate represents the estimate of effect, standard error represents the 95% confidence interval, and the *p*-value represents the statistical significance with statistically significant values indicate by an asterisk (*).

Variable	Estimate	Standard error	*p* -value
Proportion of bees in the top box	0.06	0.02	0.01*
Proportion of honey in the top box	-0.08	0.04	0.06*

3.3.2 Inner lid in place

The average temperature of colonies with only the inner lid in place was 20.8°C. When backward stepwise regression was applied to the average temperatures of colonies with the only the inner lid, the global model indicated that proportion of adult bees in the top box was the least significant, and thus it was removed (*p*-value = 0.73) (Table 3.4). The next model included the amount of adult bees, amount of brood, proportion of brood in the top box, and the proportion of honey in the top box. All variables in this model were significant, and thus the final model was identified (Table 3.5). The r-squared value of this model was 0.64 and the *p*-value was 0.02.

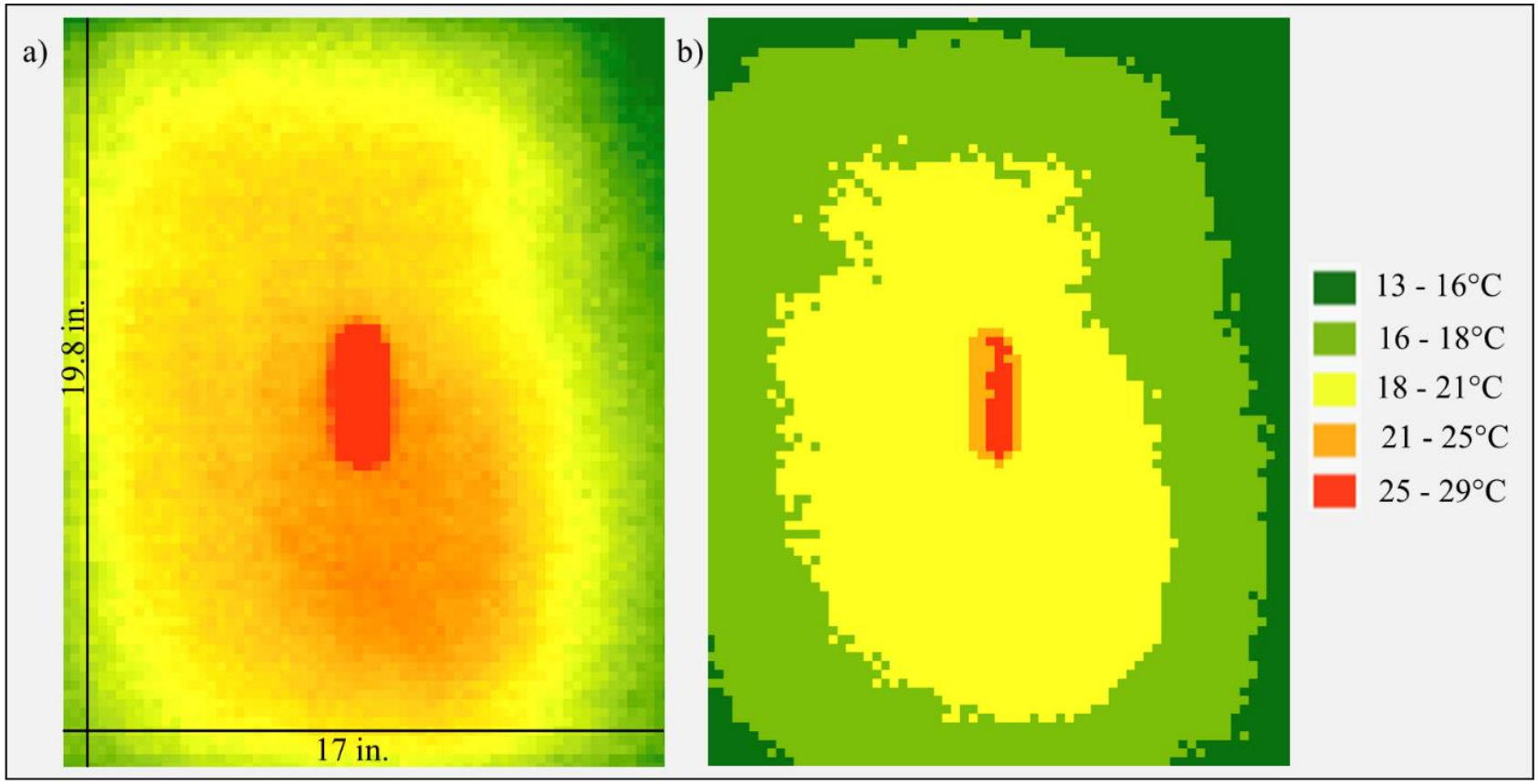

Figure 3.3 Thermal images of honey bee (*Apis mellifera*) colony one with the inner lid in place. Thermal images of colony one with the inner lid in place with the raw image (a), and the transformed image (b). In both images dark green represents 13-17°C, light green represents 17-20°C, yellow represents 20-22°C, orange represents 22-25°C, and red represents 25-30°C. Each colony had standard dimensions and measures 19.8 inches by 17 inches. Each colony had standard dimensions and measures 19.8 inches by 17 inches. The inner lid has a small hole in the middle, which can be seen in red in both images.

Table 3.4 Inner lid in place global model results. Variable represents all variables included in the model, estimate represents the estimate of effect, standard error represents the 95% confidence interval, and the *p*-value represents the statistical significance with statistically significant values indicate by an asterisk (*).

Variable	Estimate	Standard error	*p* -value
Sides of adult bees	-0.27	0.12	0.05*
Sides of brood	0.44	0.29	0.16
Proportion of adult bees in the top box	0.008	0.023	0.73
Proportion of brood in the top box	0.015	0.015	0.4
Proportion of honey in the top box	-0.051	0.023	0.05*

Table 3.5 Inner lid final model results. Variable represents all variables included in the model, estimate represents the estimate of effect, standard error represents the 95% confidence interval, and the *p*-value represents the statistical significance with statistically significant values indicate by an asterisk (*).

Variable	Estimate	Standard error	*p* -value
Sides of adult bees	-0.3	0.08	0.003*
Sides of brood	0.5	0.23	0.05*
Proportion of brood in the top box	0.02	0.008	0.04*
Proportion of honey in the top box	-0.05	0.022	0.04*

3.3.3 Neither lid in place

The average temperature of colonies with no lid was 23.3°C. When backward stepwise regression was applied to the average temperatures of colonies with no lids, the global model indicated that the amount of adult bees was the least significant, and thus it was removed from further models (*p*-value = 0.89) (Table 3.6). The next model included amount of brood, proportion of adult bees in the top box, proportion of brood in the top box, and proportion of honey in the top box. The next model indicated that the proportion of honey in the top box was the least significant, and thus it was removed (*p*-value = 0.89) (Table 3.7). The next model included the amount of brood, proportion of brood in the top box, and the proportion of adult bees in the top box. This model indicated that the proportion of adult bees in the top box was the

least significant, and thus it was removed (*p*-value = 0.36) (Table 3.8). The next model included the amount of brood, and the proportion of brood in the top box. This model indicated that the amount of brood was not significant, and thus it was removed (*p*-value = 2.1) (Table 3.9). The next model included the proportion of brood in the top box and was found to be significant (Table3.10). Additionally, the estimate of effect of the proportion of brood in the top box did not significantly changed, thus indicating that the amount of brood is not a confounding variable. This was further confirmed with a VIF score of 1.01, which indicated no correlation between the two variables.

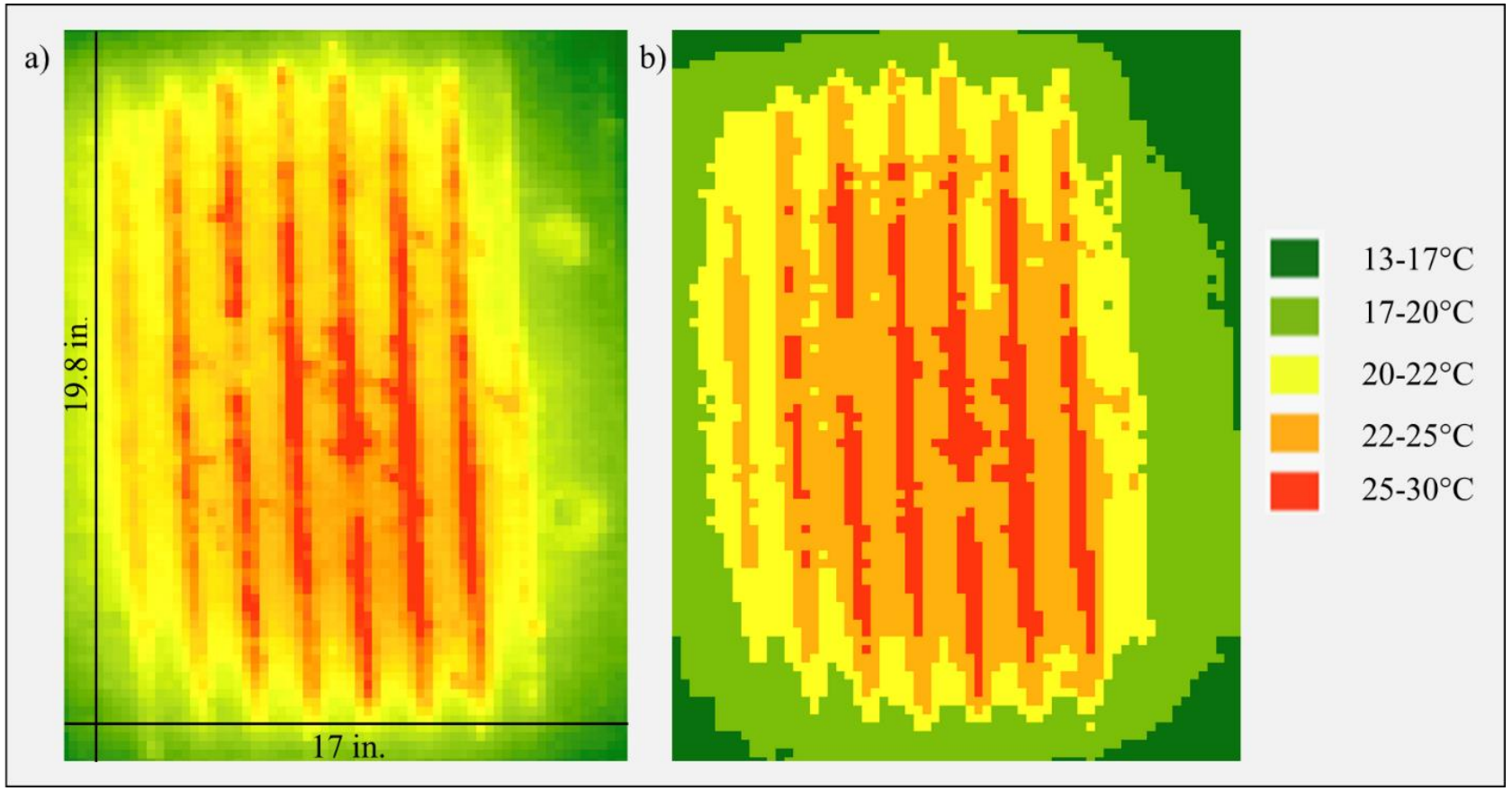

Figure 3.4 Thermal image of honey bee (*Apis mellifera*) colony one with neither lid in place. Thermal images of colony one with neither lid in place with the raw image (a), and the transformed image (b). In both images dark green represents 13-17°C, light green represents 17-20°C, yellow represents 20-22°C, orange represents 22-25°C, and red represents 25-30°C. Each colony had standard dimensions and measures 19.8 inches by 17 inches. The colony feeder can be seen in light green on the right side of image a. Additionally, hive frames can be seen in both images in orange with the space in between frames in red where adult bees occur.

Table 3.6 No lid global model results. Variable represents all variables included in the model, estimate represents the estimate of effect, standard error represents the 95% confidence interval, and the *p*-value represents the statistical significance with statistically significant values indicate by an asterisk (*).

Variable	Estimate	Standard error	*p* -value
Sides of adult bees	-0.02	0.11	0.89
Sides of brood	0.25	0.25	0.35
Proportion of adult bees in the top box	0.01	0.02	0.69
Proportion of brood in the top box	0.01	0.01	0.41
Proportion of honey in the top box	-0.29	0.02	0.89

Table 3.7 No lid second model results. Variable represents all variables included in the model, estimate represents the estimate of effect, standard error represents the 95% confidence interval, and the *p*-value represents the statistical significance with statistically significant values indicate by an asterisk (*).

Variable	Estimate	Standard error	*p* -value
Sides of brood	0.22	0.18	0.35
Proportion of adult bees in the top box	0.01	0.01	0.69
Proportion of brood in the top box	0.01	0.01	0.41
Proportion of honey in the top box	-0.002	0.02	0.89

Table 3.8 No lid third model results. Variable represents all variables included in the model, estimate represents the estimate of effect, standard error represents the 95% confidence interval, and the *p*-value represents the statistical significance with statistically significant values indicate by an asterisk (*).

Variable	Estimate	Standard error	*p* -value
Sides of brood	0.23	0.16	0.18
Proportion of adult bees in the top box	0.01	0.01	0.36
Proportion of brood in the top box	0.01	0.01	0.23

Table 3.9 No lid fourth model results. Variable represents all variables included in the model, estimate represents the estimate of effect, standard error represents the 95% confidence interval, and the *p*-value represents the statistical significance with statistically significant values indicate by an asterisk (*).

Variable	Estimate	Standard error	*p* -value
Sides of brood	0.21	0.16	0.21
Proportion of brood in the top box	0.02	0.01	0.02*

Table 3.10 No lid final model results. Variable represents all variables included in the model, estimate represents the estimate of effect, standard error represents the 95% confidence interval, and the *p*-value represents the statistical significance with statistically significant values indicate

Variable	Estimate	Standard error	*p* -value
Proportion of brood in the top box	0.02	0.01	0.01*

3.4 Discussion

3.4.1 Inner and outer lid in place

When the inner and outer lid were left in place the final model indicated that the proportion of adult bees in the top box was positively correlated with the average colony temperature and the proportion of honey in the top box was negatively correlated with the average colony temperature. This model indicates that as the proportion of adult bees in the top box increases, the average colony temperature also increases. Conversely, as the proportion of honey in the top box increase, the average colony temperature decreases. When these results are compared to Shaw et al. (2010) the positive correlation between proportion of adult bees in the top box and average colony temperature shown here is similar to the positive correlation between the amount of adult bees and average colony temperature shown in Shaw et al. (2010). Proportion of adult bees in the top box was likely more significant than the amount of adult bees because the thermal images captured were taken from above, and thus the thermal signature of the top of the colony is accurately measured. Similarly, the proportion of honey in the top box was likely more significant than the amount of honey because the thermal images were again taken from above. The positive correlation between the proportion of adult bees in the top box indicates that when a thermal image is taken from above with the inner and outer lid in place the proportion of adult bees in the top box can be estimated. Additionally, the negative correlation between the

proportion of honey in the top box indicates that when a thermal image is taken from above with the inner and outer lid in place the proportion of honey in the top box can be determined.

The statistical non-significance of the amount of bees, brood, and proportion of brood in the top box indicates that they do not contribute to the average colony temperature. When compared with the results of Shaw et al. (2010) the statistical non-significance between the amount of adult bees and average colony temperature shown here is contradictory to the positive correlation between the amount of adult bees and average colony temperature shown in Shaw et al. (2010). However, this is likely because Shaw et al. (2010) captured images from in front and behind the colony where the thickness of the hive is smaller. Additionally, the average colony temperature with both lids in place was on average significantly lower than when the inner lid was in place and when no lid was in place. This is likely because the outer lid is wrapped in a metal sheet and thus reflects the thermal signature of the environment rather than indicating the thermal signature of the colony.

3.4.2 Inner lid in place

When the inner lid was left in place the final model indicated that the amount of adult bees, brood, proportion of brood in the top box, and the proportion of honey in the top box significantly contributed to the average colony temperature. Specifically, the amount of adult bees was slightly negatively correlated with the average colony temperature. This indicates that as the amount of adult bees increases, the average colony temperature slightly declines. Additionally, the proportion of honey in the top box was also negatively correlated with the average colony temperature. This indicates that as the proportion of honey in the top box increases, the average colony temperature declines. Conversely, the amount of brood was positively correlated with the average colony temperature. This indicates that as the amount of

brood increases, the average colony temperature also increases. Additionally, the proportion of honey in the top box was also positively correlated with the average colony temperature. This indicates that as the proportion of brood in the top box increases, the average colony temperature also increases.

When the negative correlation between the amount of bees and the average colony temperature is compared to Shaw et al. (2010) the opposite trend is seen. The opposing trends among the amount of adult bees and the average colony temperature is likely a result of the differing thermal image angles. Thermal images taken from above the colony may only capture the thermal signature of adult bees in the top box, while images taken from in front and behind the colony may capture the thermal signature of adult bees throughout the colony. However, the statistical significance of the amount of brood, the proportion of brood in the top box, and the proportion of honey in the top box indicates that they significantly contribute to the average colony temperature, and thus should be included in investigations of average colony temperature. The statistical non-significance of the proportion of adult bees in the top box indicates that the proportion of adult bees in the top box does not significantly contribute to the average colony temperature. This may be because the statistical significance of all other variables may mask more minute trends.

3.4.3 Neither lid in place

When the inner lid was left in place the final model indicated that the proportion of brood in the top box significantly contributed to the average colony temperature. Specifically, the proportion of brood in the top box was positively correlated with the average colony temperature. This indicates that when neither lid is in place, as the proportion of brood in the top box increase, the average colony temperature also increases.

The statistical non-significance of the amount of bees, brood, the proportion of adult bees in the top box, and proportion of honey in the top box indicates that when both lids are removed these variables do not contribute to the average colony temperature. This may be because the removal of hive lids disrupts colony activity, and thus the amount of bees, brood, and position of adult bees and honey may appear to change.

3.4.4 Significance of research for geospatial investigations

These results are significant for geospatial research because it is the first indication that a drone equipped with a thermal sensor is applicable in honey bee systems to measure average colony temperature. Further geospatial investigations within honey bee systems may apply drone technology to map bee yards and identify optimal colony placement.

3.4.5 Significance of research for beekeepers

The results shown here are significant for beekeepers because the use of a drone equipped with a thermal sensor may reduce the amount of labor and time required to estimate honey bee colony health. With the amount of labor and time required to estimate honey bee colony health reduced, honey bee colony health surveys can be completed more regularly. When variables of honey bee colony health are estimated more often, more informed management decisions can be made by beekeepers, which then decreases the rate of honey bee colony loss.

Commercial beekeepers (beekeepers with 300 or more colonies) are most likely to benefit from more efficient thermal colony health surveys conducted by a drone because they have more colonies to survey, and are required to report the health of their colonies prior to pollination of agricultural crops. Additionally, commercial honey bee colonies have a single lid that closely resembles the inner lid of backyard beekeeper colonies, and thus no lid would need to be removed for thermal colony health surveys conducted by drone.

3.4.6 Limitations

This research was limited in that the drone could not be flown as a result of local ordinance. Although if the drone is flown at a similar height to where it was held (~1 meter) the results should be similar, however, this can not be confirmed until investigations have completed similar analysis while flying the drone. Furthermore, this research was limited in sample size. Although 47 colonies were manually surveyed, only 15 were sampled using thermal analysis. The limited sample size was a result of preliminary testing, and thus larger sample sizes should be collected and analyzed in the future. This analysis was also limited in the temporal scope. All thermal images were taken on the same day under the same environmental conditions, however, environmental conditions may alter these results, and thus this analysis should be repeated under varying environmental conditions to estimate its effect.

3.4.7 Future research

Future research should investigate the time in between manual inspection and thermal surveys to determine when thermal surveys should be conducted and how long they will remain accurate after manual colony inspection. Future research should also investigate further metrics of honey bee colony health. The inner lid model explained 64% of the variance in the average colony temperature, which indicates that there are several variables that significantly contribute to the average colony temperature that were not included in this model. These variables may include ambient temperature (Farenhotlz et al. 1989), genetic diversity of the colony (Jones et al. 2004), and the population of drones within the colony (Coelho 1991).

3.5 Conclusion

Elevated rates of honey bee colony loss in the United States have underscored the importance of regular colony inspections as they can provide early warning signs of colony loss. Here I have

shown that a drone equipped with a thermal sensor can be used to measure the average colony temperature with the inner lid in place, and that the amount of adult bees, brood, and position of brood and honey significantly contribute to the average colony temperature. These results are significant because they provide the first indication that a drone equipped with a thermal sensor can provide a more efficient method for estimating honey bee colony health. When honey bee colony health is measured more regularly, more informed management decisions can be applied by beekeepers, and thus the likelihood of colony loss is reduced.

3.6 References

Braga, A.R., D.G. Gomes, R. Rogers, E.E. Hassler, B.M. Freitas, J.A. Cazier. 2020. "A method for mining combined data from in-hive sensors, weather and apiary inspections to forecast the health status of honey bee colonies." Computers and Electronics in Agriculture 169, 105161. DOI: https://doi.org/10.1016/j.compag.2019.105161.

Bruckner, S., N. Steinhauer, J. Engelsma, A.M. Fauvel, K. Kulhanek, E. Malcolm, A. Meredith, M. Milbrath, E.L. Niño, J. Rangel, K. Rennich, D. Reynolds, R. Sagili, J. Tsuruda, D. vanEngelsdorp, S.D. Aurell, M. Wilson, G. Williams. 2020. "2019-2020 Honey Bee Colony Losses in the United States: Preliminary Results."

Dainat, B., J.D. Evans, Y.P. Chen, L. Gauthier, P. Neumann. 2012. "Predictive Markers of Honey Bee Colony Collapse." PLoS ONE 7, e32151. DOI: https://doi.org/10.1371/journal.pone.0032151.

Daponte, P., L. De Vito, L. Glielmo, L. Iannelli, D. Liuzza, F. Picariello, G. Silano. 2019. "A review on the use of drones for precision agriculture." IOP Conference Series: Earth Environmental Science 275, 012022. DOI: https://doi.org/10.1088/1755-1315/275/1/012022.

Delaplane, K.S., J. van der Steen, E. Guzman-Novoa. 2013. "Standard methods for estimating strength parameters of *Apis mellifera* colonies." Journal of Apicultural Research 52, 1-12. DOI: https://doi.org/10.3896/IBRA/1.52.1.03.

Efroymson, M.A., 1960. "Multiple regression analysis." Mathematical methods for digital computers, pp.191-203.

Fahrenholz, L., I. Lamprecht, B. Schricker. 1989. "Thermal investigations of a honey bee colony: thermoregulation of the hive during summer and winter and heat production of members of different bee castes." Journal of Comparative Physiology B 159, 551–560. DOI: https://doi.org/10.1007/BF00694379

Jones, J.C., M.R. Myerscough, S. Graham, B.P. Oldroyd. 2004. "Honey Bee Nest Thermoregulation: Diversity Promotes Stability." Science 305, 402–404. DOI : https://doi.org/10.1126/science.1096340

Klein, A.-M., B.E. Vaissière, J.H. Cane, I. Steffan-Dewenter, S.A. Cunningham, C. Kremen, T. Tscharntke. 2007. "Importance of pollinators in changing landscapes for world crops." Proceedings of the Royal Society B: biological sciences 274, 303–313. DOI: https://doi.org/10.1098/rspb.2006.3721.

Kulhanek, K., N. Steinhauer, K. Rennich, D.M. Caron, R.R. Sagili, J.S. Pettis, J.D. Ellis, M.E. Wilson, J.T. Wilkes, D.R. Tarpy, R. Rose, K. Lee, J. Rangel & D. vanEngelsdorp. 2017. "A national survey of managed honey bee2015–2016 annual colony losses in the USA." Journal of Apicultural Research 56 (4): 328-340. DOI: https://doi.org/10.1080/00218839.2017.1344496.

Lim, H.Y., J.G. Lee, S.B. Lee, O.M. Lee, B. Yoon. 2013. “Application of Digital Infrared Thermal Imaging (DITI) as a diagnostic method for the fate of honey bee colonies.” Journal of Apiculture 28 (2): 147-153.

Oldroyd, B.P. 2007. “What’s Killing American Honey Bees?” PLoS Biology 5(6): 1195-1199. DOI: https://doi.org/10.1371/journal.pbio.0050168.

Pierce, F.J., P. Nowak. 1999. “Aspects of Precision Agriculture, in: Advances in Agronomy.” Elsevier, pp. 1–85. DOI: https://doi.org/10.1016/S0065-2113(08)60513-1.

Shaw, J.A., P.W. Nugent, J. Johnson, J.J. Bromenshenk, C.B. Henderson, S. Debnam. 2011. “Long-wave infrared imaging for non-invasive beehive population assessment.” Optics Express 19, 399. DOI: https://doi.org/10.1364/OE.19.000399.

Stabentheiner, A., H. Pressl, T. Papst, N. Hrassnigg, K. Crailsheim. 2003. “Endothermic heat production in honeybee winter clusters.” Journal of Experimental Biology, 206(2), pp.353-358.

Stehr, N.J. 2015. “Drones: The Newest Technology for Precision Agriculture.” Natural Sciences Education 44, 89–91. DOI: https://doi.org/10.4195/nse2015.04.0772.

Svatos, M.K., and MG. Trowbridge. 2018. “Australian Drone Technology Assisting a Significant Step in Crop Tolerance to Heat and Drought Stress” Future Directions international 1-5.

Thompson, B. 1995. “Stepwise regression and stepwise discrimant analysis need not apply here: a guidelines editorial.” Educational and Psycholoigcal Measurement 55(4), 525-534.

Zacepins, A., E. Stalidzans, and J. Meitalovs. 2012. “Application of information technologies in precision apiculture.” In Proceedings of the 13th International Conference on Precision Agriculture (ICPA 2012).